Effects of Collision Dynamics on pϕ Femtoscopy

arXiv:2410.01204 [hep-ph]

SOPHIA U

SOPHIA HADRON PHYSICS GROUP

Kenshi Kuroki (Sophia University, JP)

k-kuroki-e23@eagle.sophia.ac.jp

In collaboration with

Tetsufumi Hirano (Sophia University, JP)

Basics of Femtoscopy

- Correlation Function
- Koonin-Pratt Formula

Hadron Correlations

Momentum correlations in **high-energy nuclear collisions**

→ Useful for studying **low-energy hadron interactions**

Correlation Function (CF) at Pair Rest Frame ($\boldsymbol{P} = 0$)

$$C(\boldsymbol{q}) := \frac{N_{\text{pair}}(\boldsymbol{p}_a, \boldsymbol{p}_b)}{N_a(\boldsymbol{p}_a)\, N_b(\boldsymbol{p}_b)}$$

Total momentum: $\boldsymbol{P} = \boldsymbol{p}_a + \boldsymbol{p}_b$

Relative momentum: $\boldsymbol{q} = \frac{m_b \boldsymbol{p}_a - m_a \boldsymbol{p}_b}{m_a + m_b}$

Two-particle momentum dist.: $N_{\text{pair}}(\boldsymbol{p}_a, \boldsymbol{p}_b)$

One-particle momentum dist.: $N_a(\boldsymbol{p}_a)$

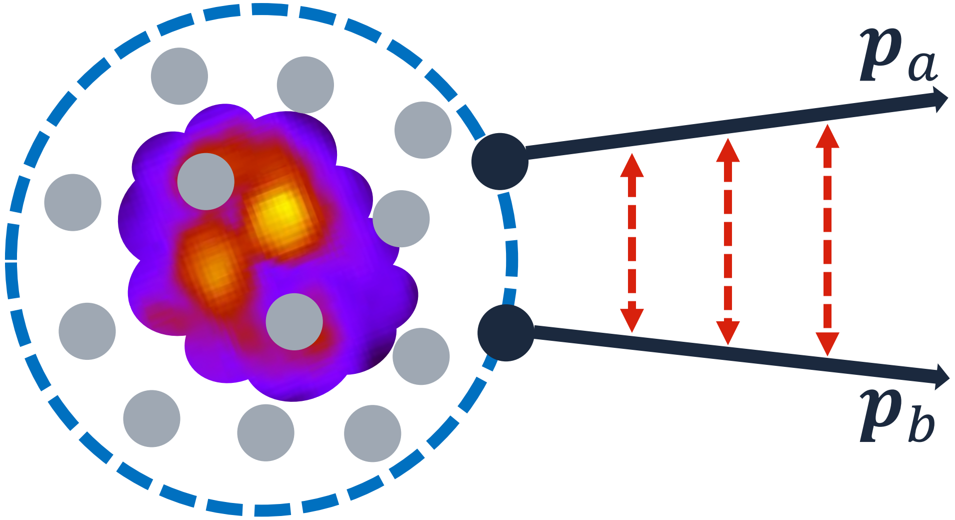

Hadron Correlations

Momentum correlations in **high-energy nuclear collisions**

$\rightarrow$ Useful for studying **low-energy hadron interactions**

Correlation Function (CF) at Pair Rest Frame ($\boldsymbol{P} = 0$)

$$C(\boldsymbol{q}) := \frac{N_{\text{pair}}(\boldsymbol{p}_a, \boldsymbol{p}_b)}{N_a(\boldsymbol{p}_a)\, N_b(\boldsymbol{p}_b)}$$

Total momentum: $\boldsymbol{P} = \boldsymbol{p}_a + \boldsymbol{p}_b$

Relative momentum: $\boldsymbol{q} = \frac{m_b \boldsymbol{p}_a - m_a \boldsymbol{p}_b}{m_a + m_b}$

Two-particle momentum dist.: $N_{\text{pair}}(\boldsymbol{p}_a, \boldsymbol{p}_b)$

One-particle momentum dist.: $N_a(\boldsymbol{p}_a)$

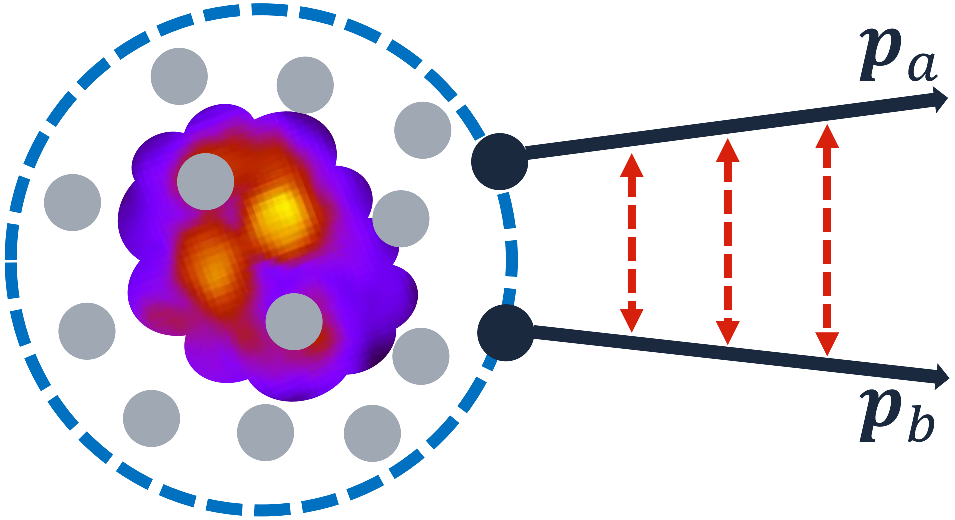

Hadron CF provides insights into

- **Space-time structure of the matter**
- **Final state hadron interactions**

Koonin-Pratt formula

S. E. Koonin, PLB **70**, 43 (1977); S. Pratt, PRL **53**, 1219 (1984)

Under several assumptions,

$$C(\boldsymbol{q}) = \int d^3r\ S(\boldsymbol{q};\boldsymbol{r})\ |\varphi(\boldsymbol{q};\boldsymbol{r})|^2$$

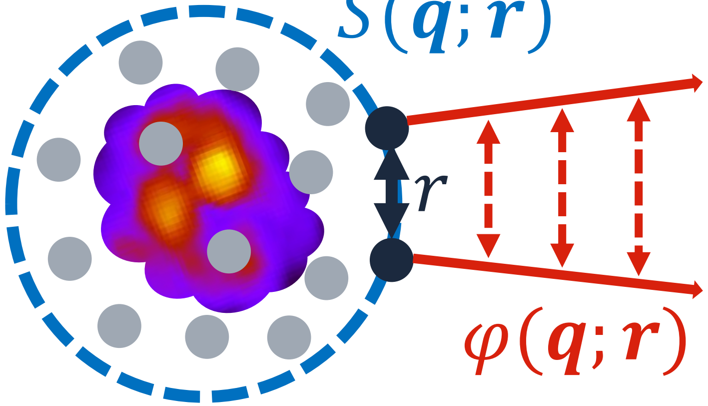

CF ⇦ **Source Func.** & **Relative WF**

Koonin-Pratt formula

S. E. Koonin, PLB **70**, 43 (1977); S. Pratt, PRL **53**, 1219 (1984)

Under several assumptions,

$$C(\boldsymbol{q}) = \int d^3r\ S(\boldsymbol{q};\boldsymbol{r})\ |\varphi(\boldsymbol{q};\boldsymbol{r})|^2$$

CF ⇦ **Source Func.** & **Relative WF**

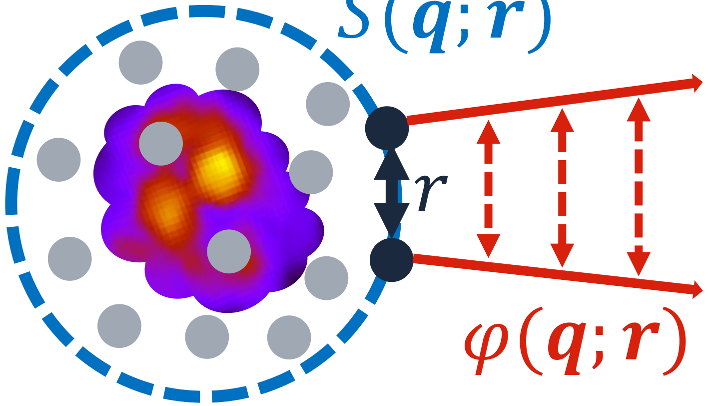

From **experimental** correlation function

- **Input**: hadron interaction → **Output**: source function
- **Input**: source function → **Output**: hadron interaction

Hadron Interaction Study via Femtoscopy

Recent active studies have demonstrated its usefulness and powerfulness

L. Fabbietti *et al.*, Ann. Rev. Nucl. Part. Sci. **71**, 377 (2021)

→ Assuming **static Gaussian SF**

Actual SF should reflect the complex dynamics of nuclear collisions

A. Ohnishi, talk at RHIC-BES On-line seminar IV (2022)

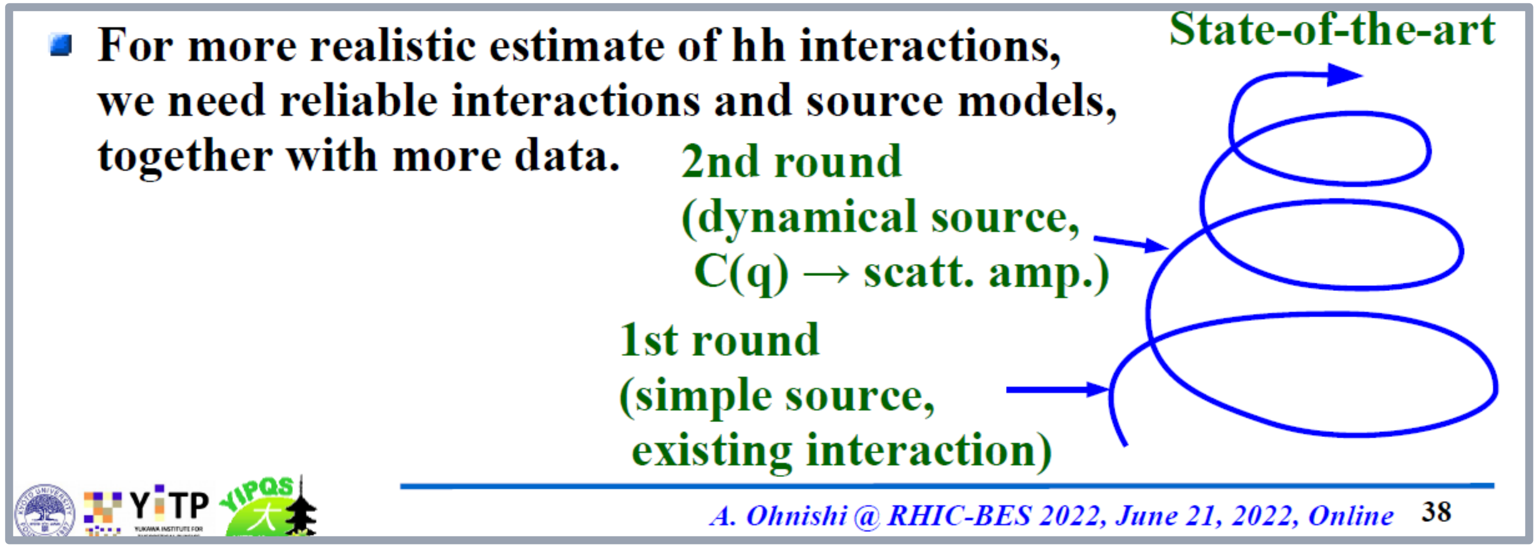

Hadron Interaction Study via Femtoscopy

Recent active studies have demonstrated its usefulness and powerfulness

L. Fabbietti *et al.*, Ann. Rev. Nucl. Part. Sci. **71**, 377 (2021)

→ Assuming **static Gaussian SF**

Actual SF should reflect the complex dynamics of nuclear collisions

A. Ohnishi, talk at RHIC-BES On-line seminar IV (2022)

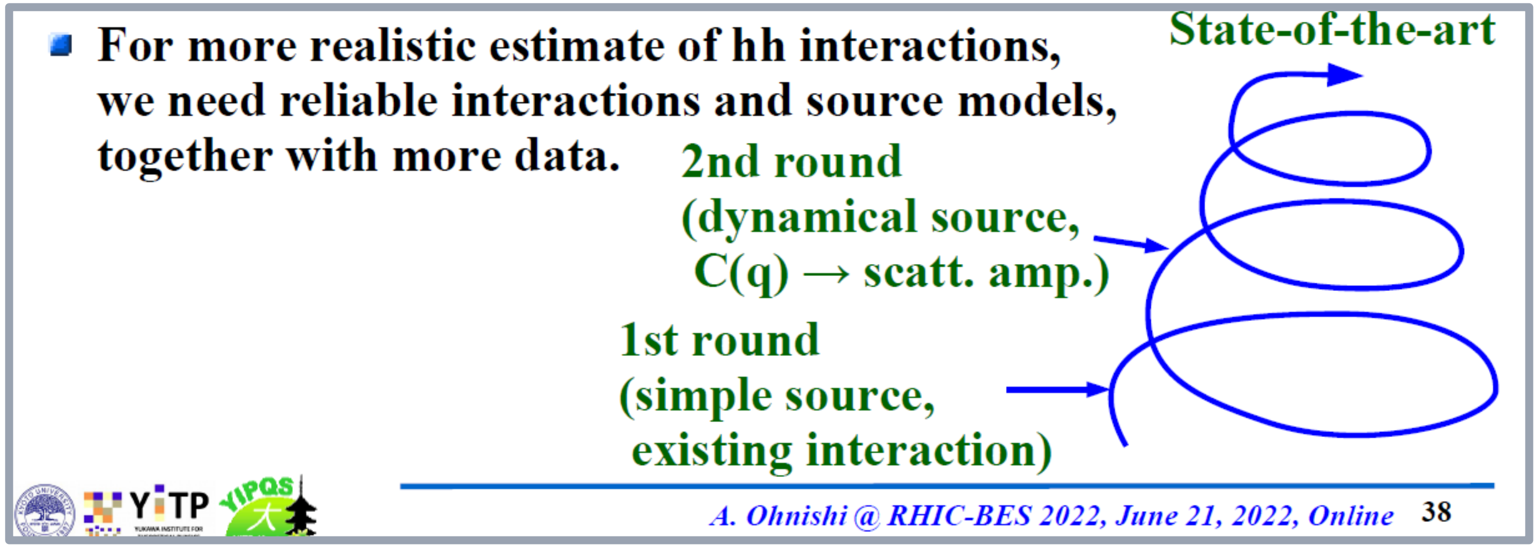

To explore less understood hadron interactions,

Femtoscopy using **dynamical models**

pϕ Femtoscopy using Dynamical Model

- Interaction
- Source Function
- Correlation Function
- Effects of Collision Dynamics

pϕ Interaction

Consider only s-wave scattering $\rightarrow$ 2 channels: ${}^4S_{3/2}$ & ${}^2S_{1/2}$

${}^4S_{3/2}$: HAL QCD potential Y. Lyu *et al.*, PRD **106**, 074507 (2022)

(2+1)-flavor lattice QCD at near physical point

➤ **Overall attraction w/o bound states**

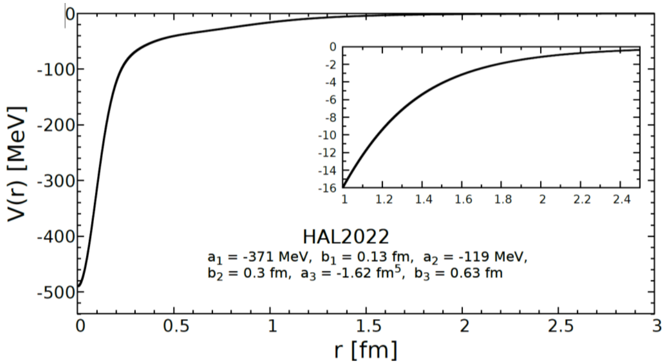

${}^2S_{1/2}$: Parametrized potential E. Chizzali *et al.*, PLB **848**, 138358 (2023)

Motivated by HAL QCD ${}^4S_{3/2}$ potential

➤ **Should be constrained phenomenologically via femtoscopy**

Femtoscopy using Gaussian SF $\rightarrow$ Indication of a bound state

Dynamical Core–Corona Initialization model (DCCI2)

Y. Kanakubo, Y. Tachibana, and T. Hirano, PRC **105**, 024905 (2022)

A cutting-edge dynamical model based on core–corona picture

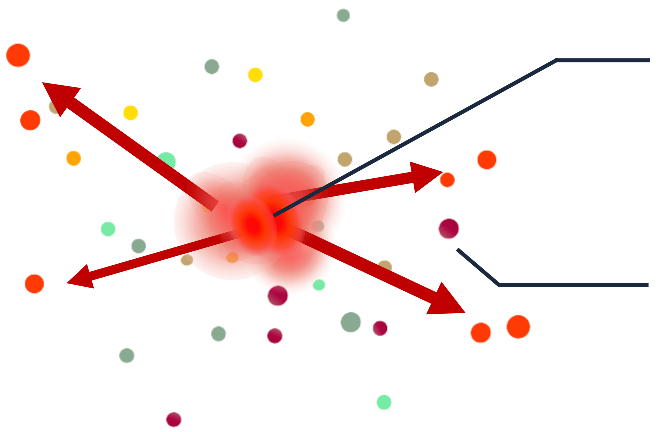

Core:
Equilibrated matter ~ QGP

Corona:
Non-equilibrium partons

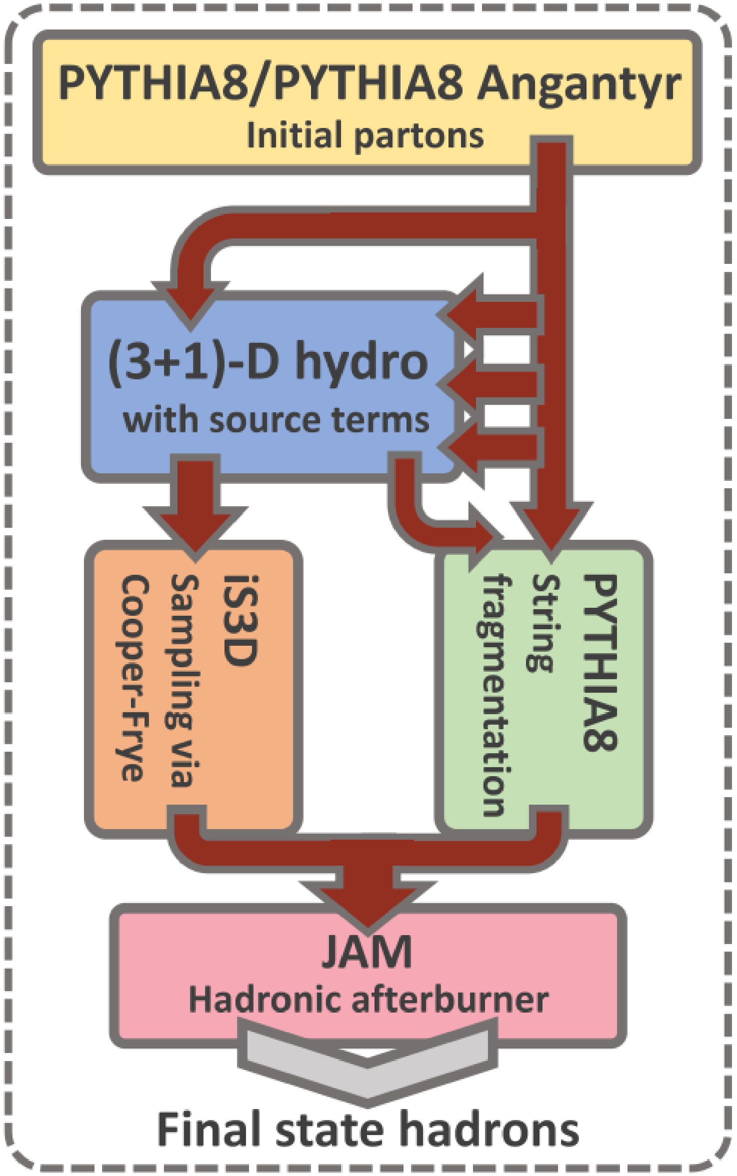

Space-Time Evolution by DCCI2

High-multiplicity p+p collisions at $\sqrt{s} = 7$ TeV

Movies provided by Y. Kanakubo

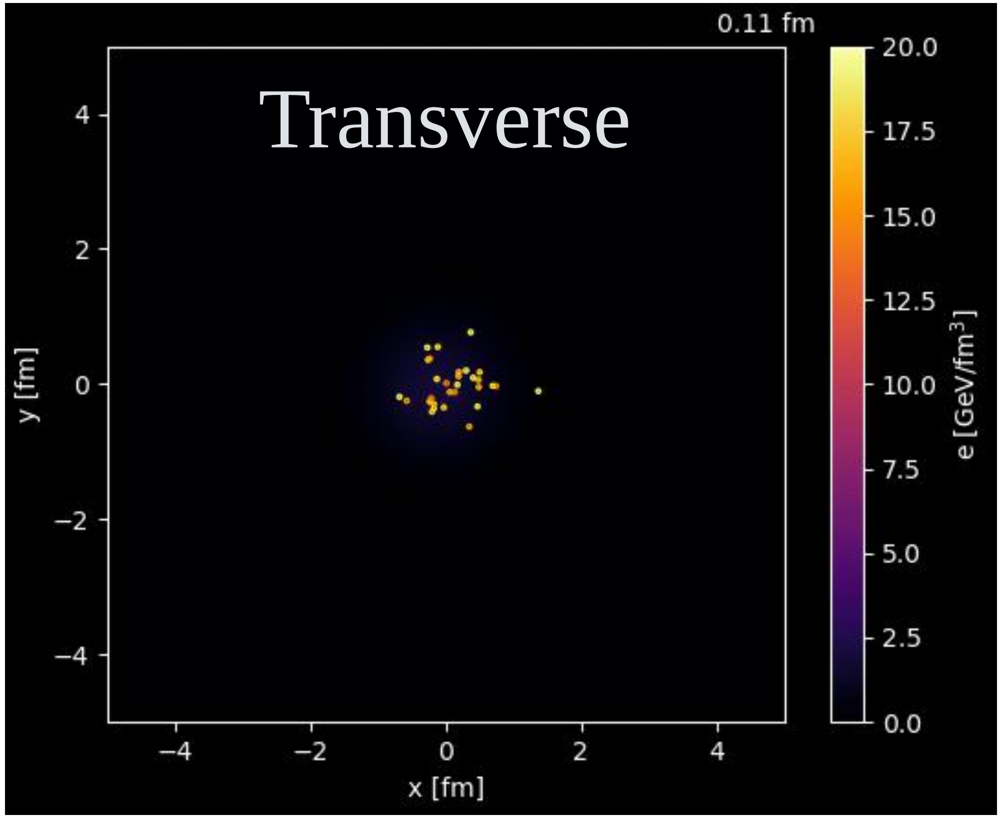

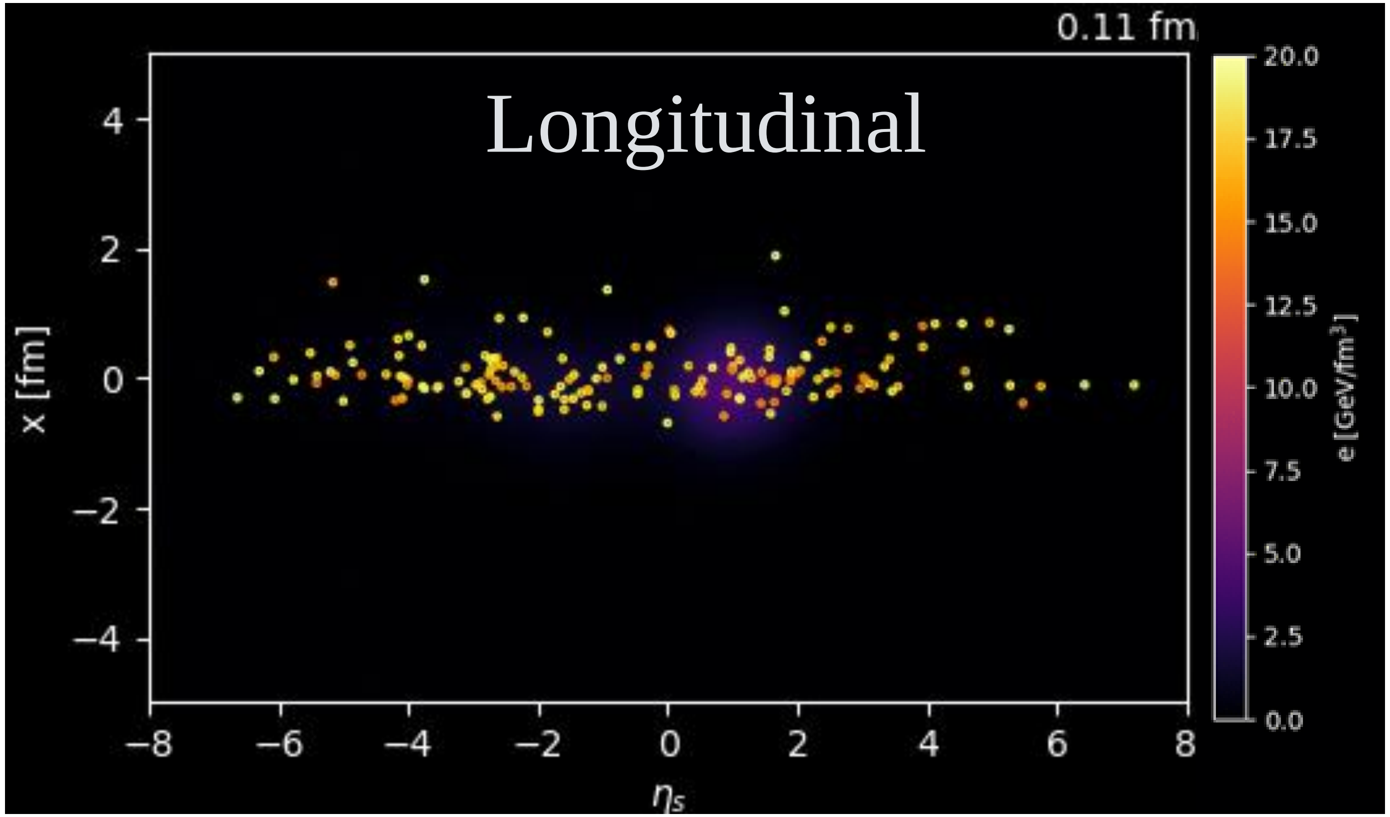

Describes the entire evolution of nuclear collisions

→ SF that reflects collision dynamics

Space-Time Evolution by DCCI2

High-multiplicity p+p collisions at $\sqrt{s} = 7$ TeV

Movies provided by Y. Kanakubo

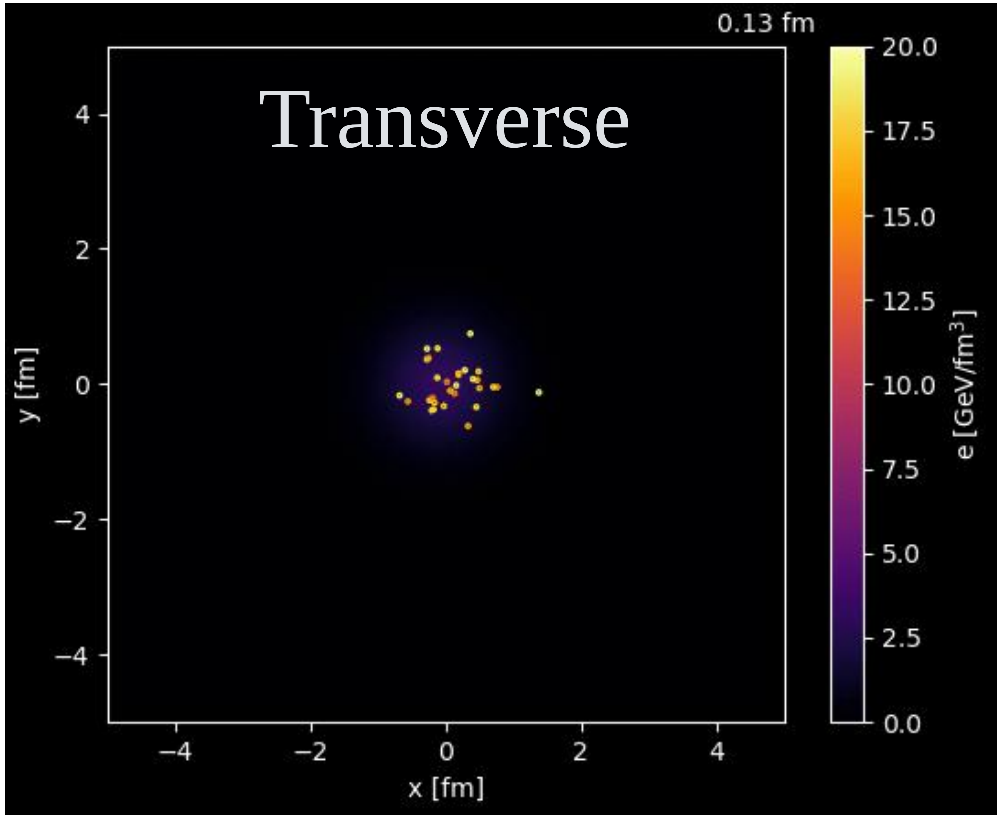

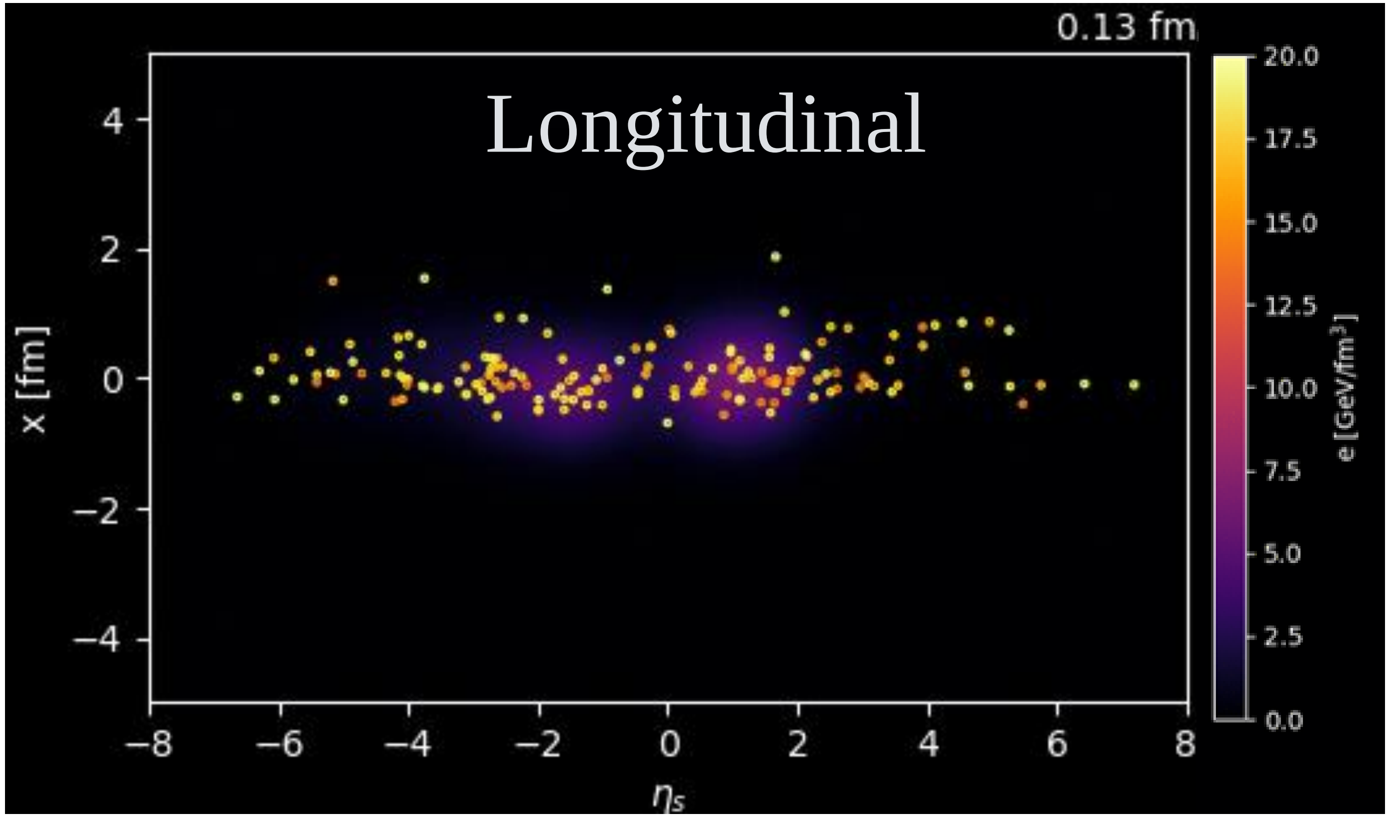

Describes the entire evolution of nuclear collisions

→ SF that reflects collision dynamics

Space-Time Evolution by DCCI2

High-multiplicity p+p collisions at $\sqrt{s} = 7$ TeV

Movies provided by Y. Kanakubo

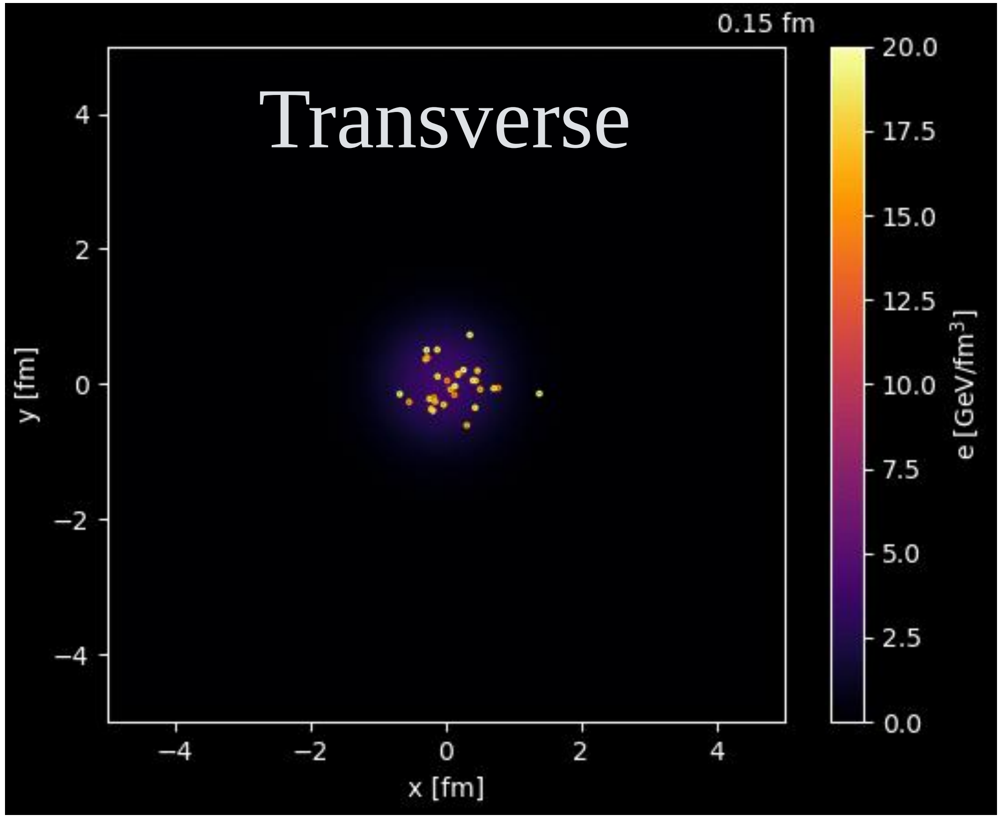

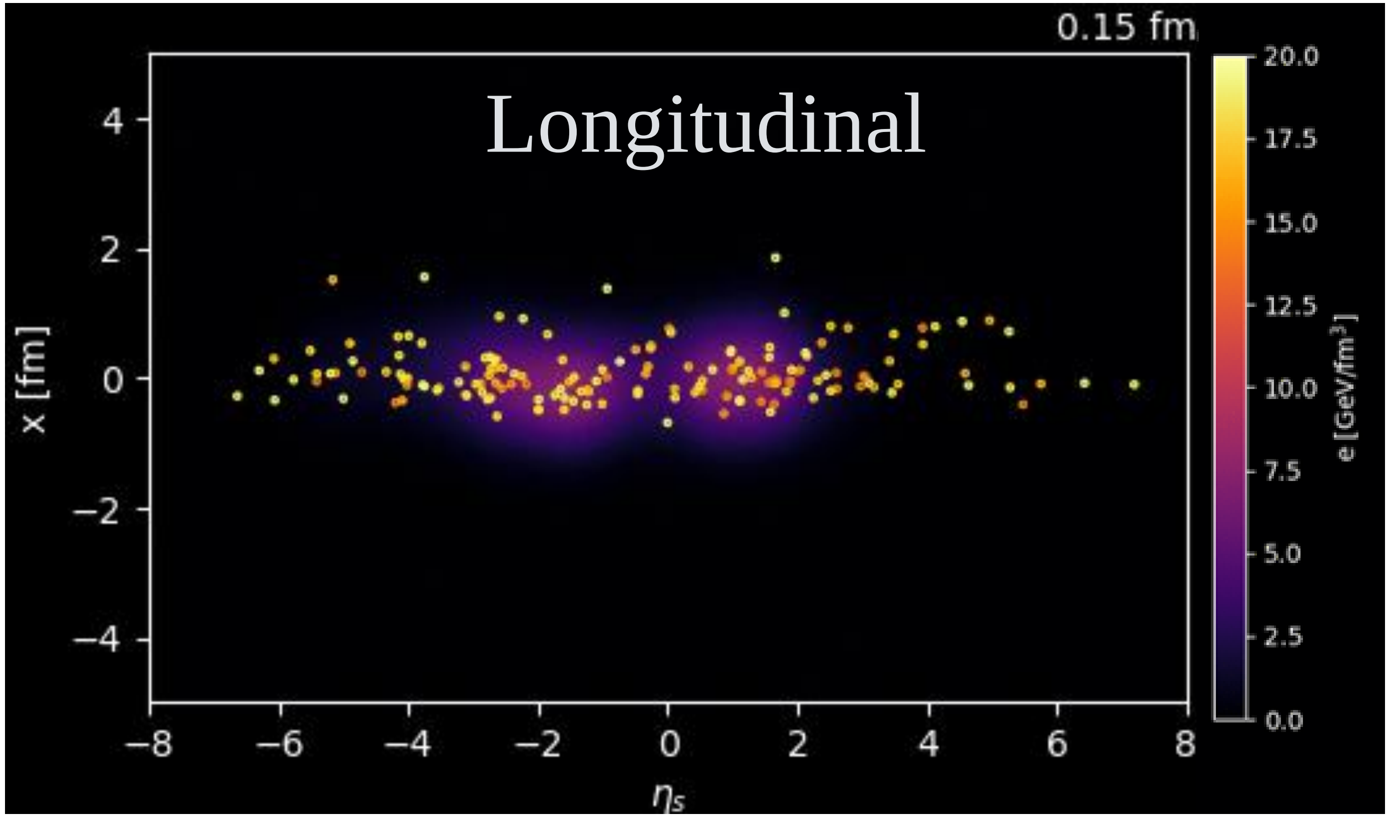

Describes the entire evolution of nuclear collisions

→ SF that reflects collision dynamics

Space-Time Evolution by DCCI2

High-multiplicity p+p collisions at $\sqrt{s} = 7$ TeV

Movies provided by Y. Kanakubo

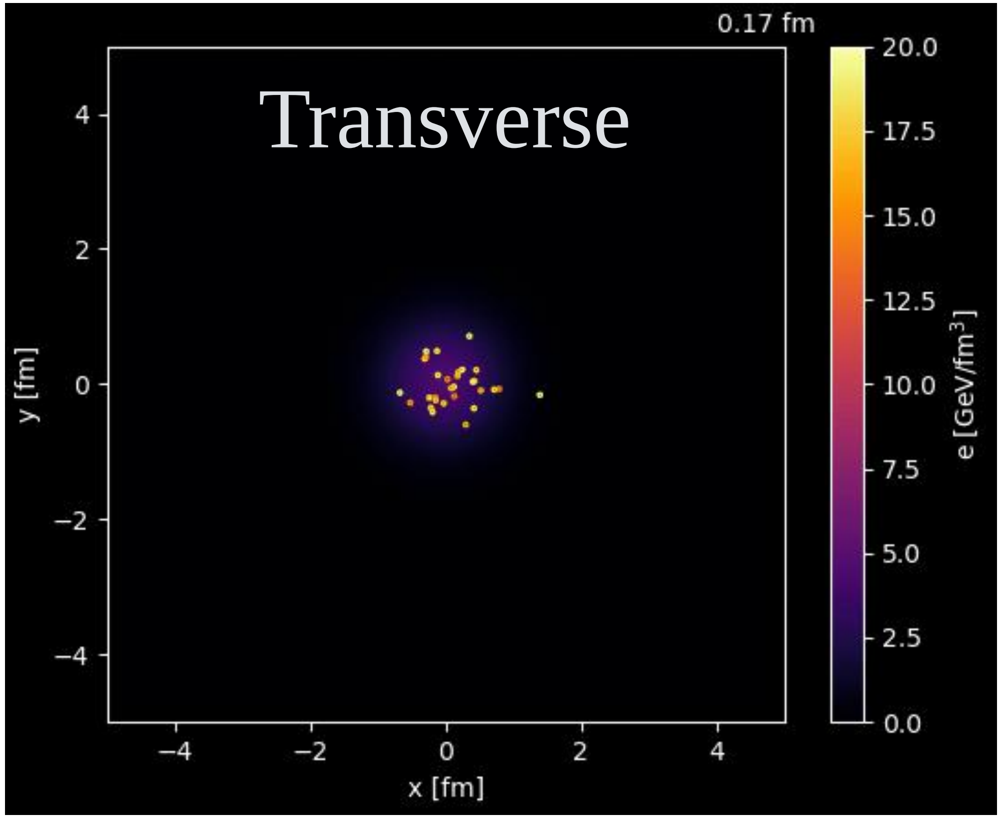

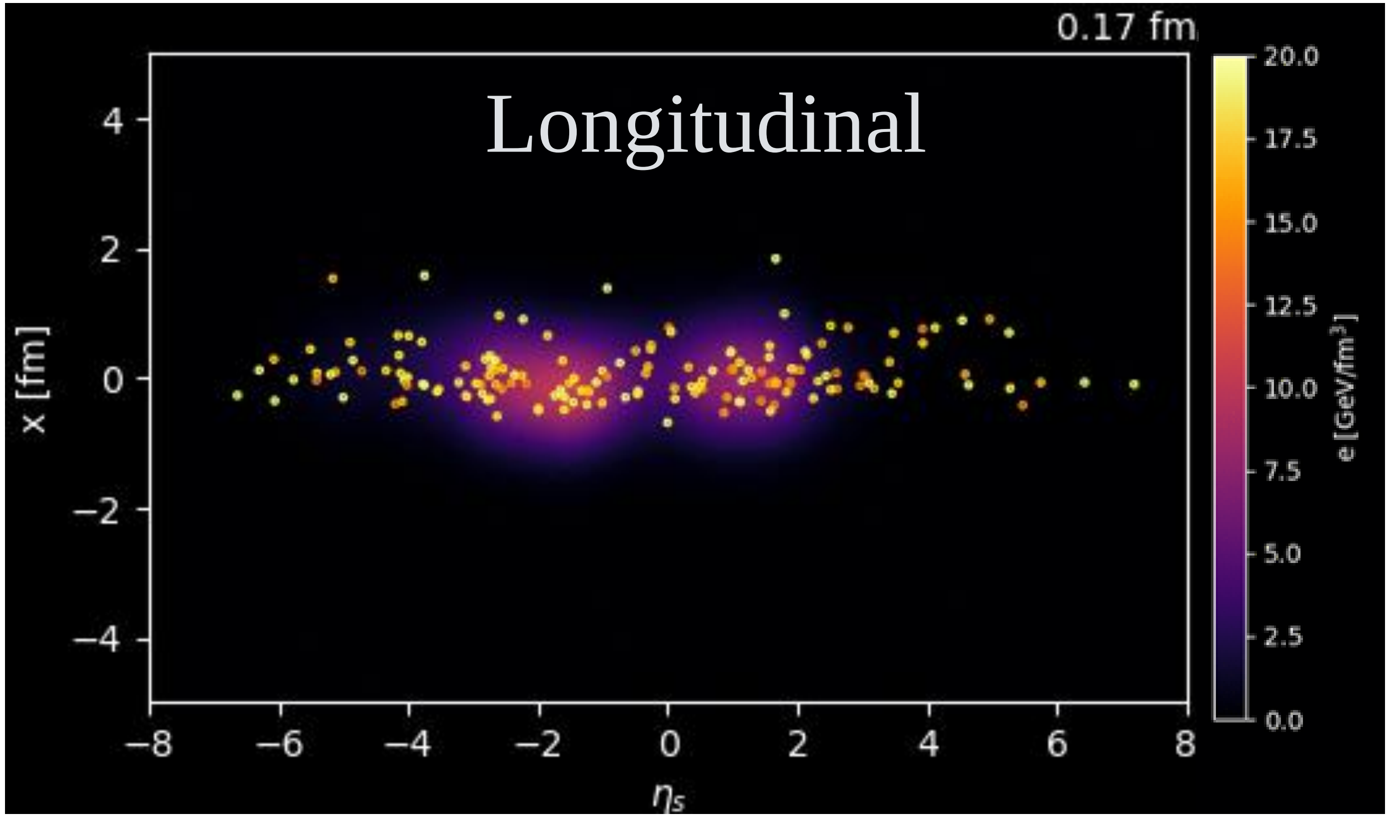

Describes the entire evolution of nuclear collisions

→ SF that reflects collision dynamics

Space-Time Evolution by DCCI2

High-multiplicity p+p collisions at $\sqrt{s} = 7$ TeV

Movies provided by Y. Kanakubo

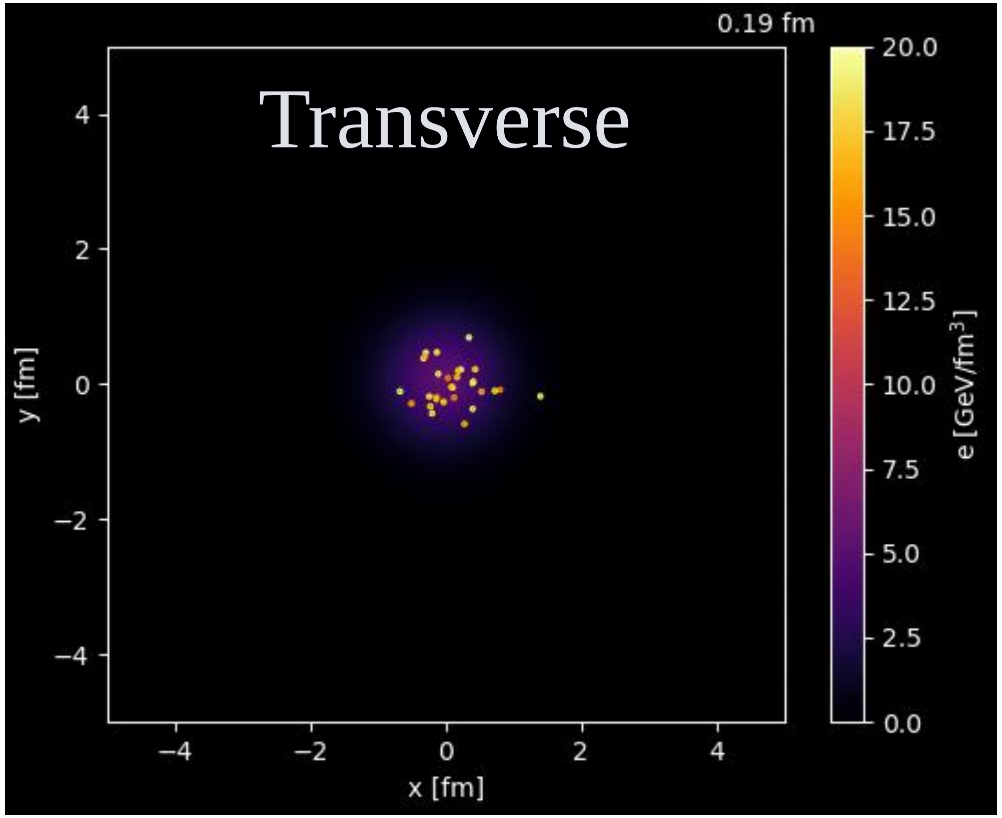

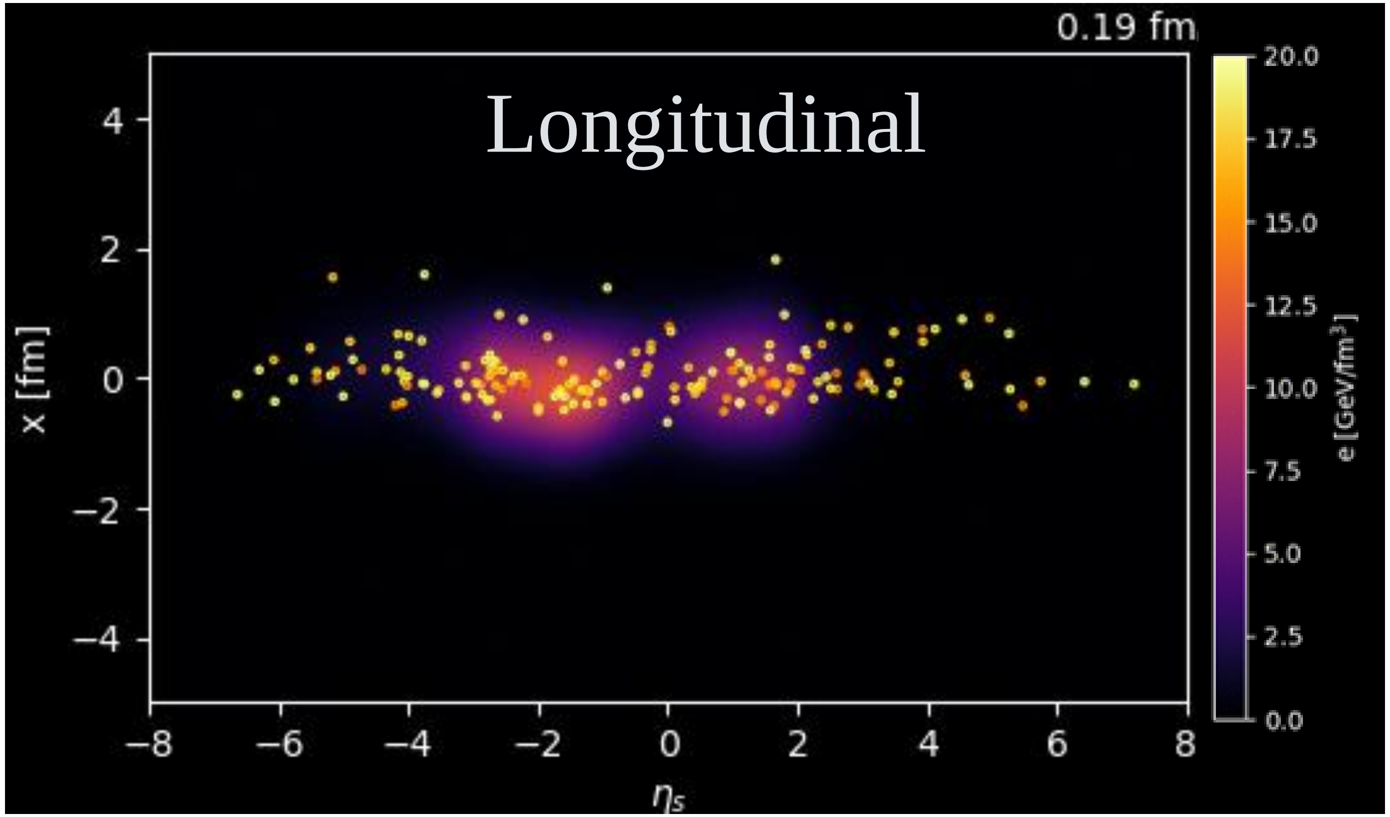

Describes the entire evolution of nuclear collisions

→ SF that reflects collision dynamics

Space-Time Evolution by DCCI2

High-multiplicity p+p collisions at $\sqrt{s} = 7$ TeV

Movies provided by Y. Kanakubo

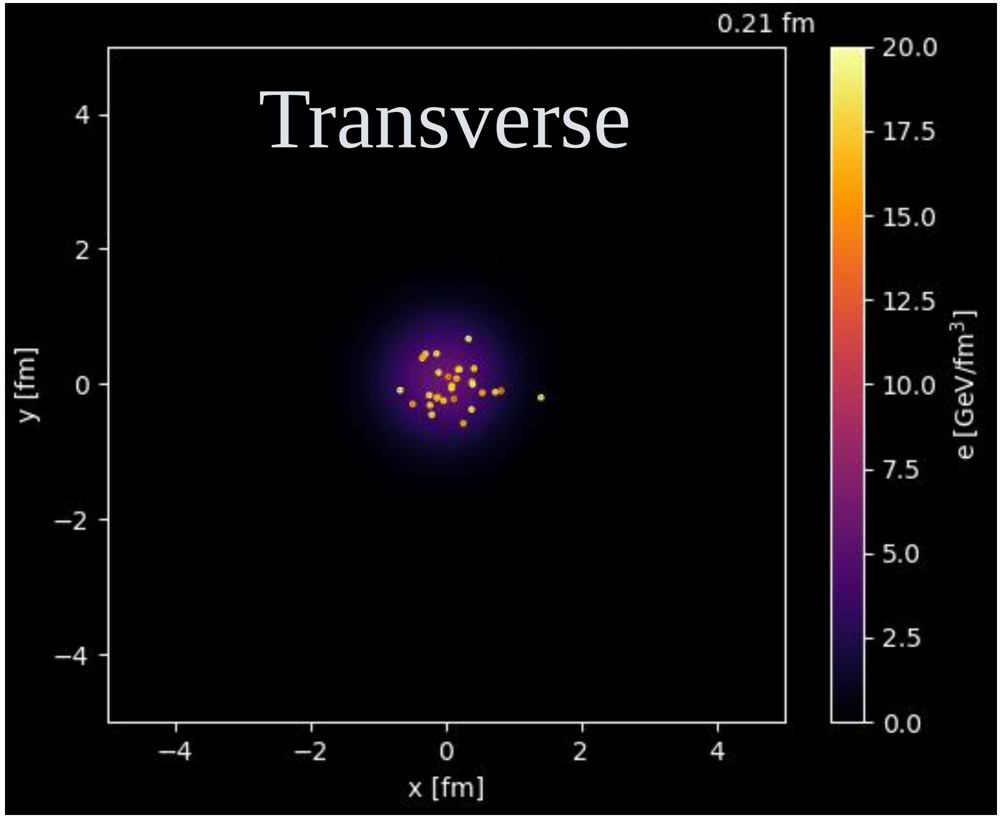

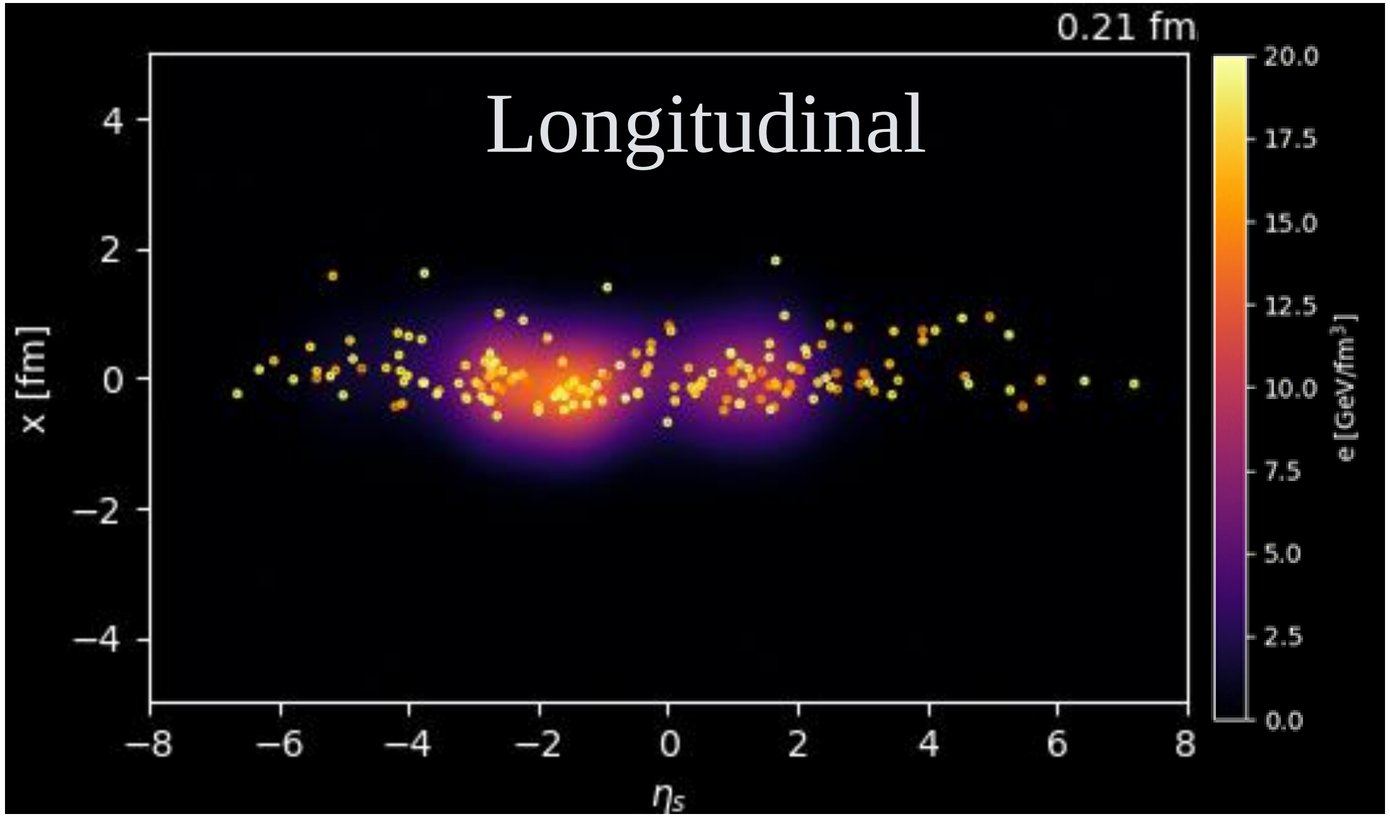

Describes the entire evolution of nuclear collisions

→ SF that reflects collision dynamics

Space-Time Evolution by DCCI2

High-multiplicity p+p collisions at $\sqrt{s} = 7$ TeV

Movies provided by Y. Kanakubo

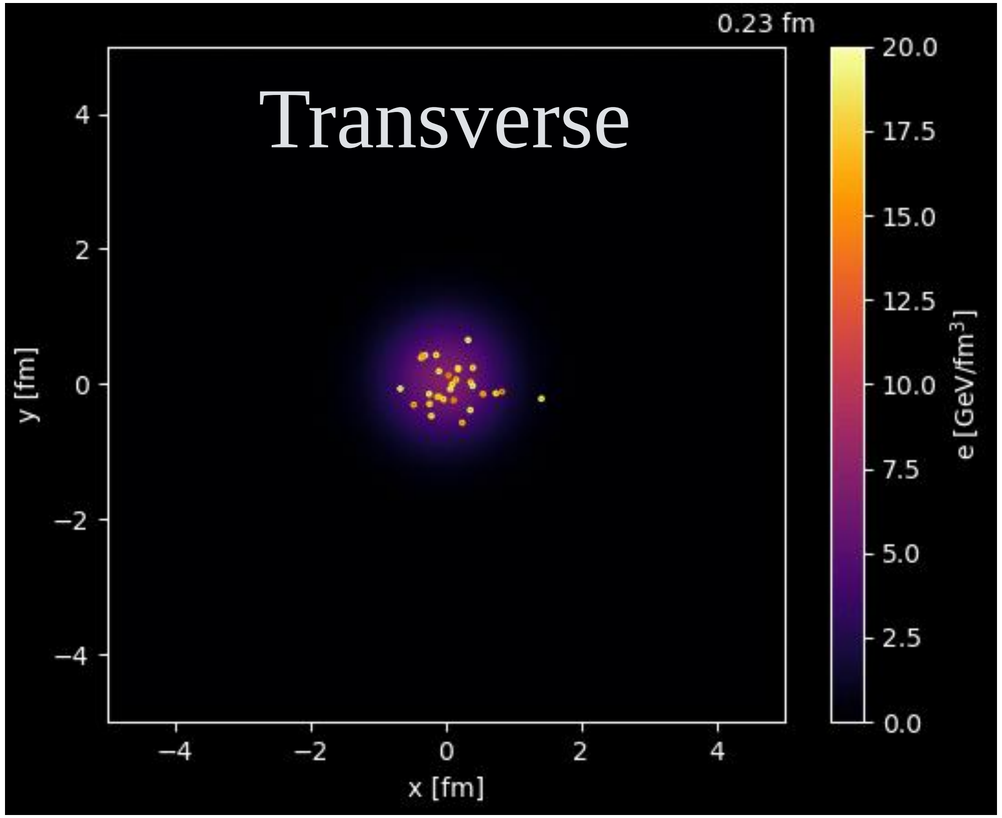

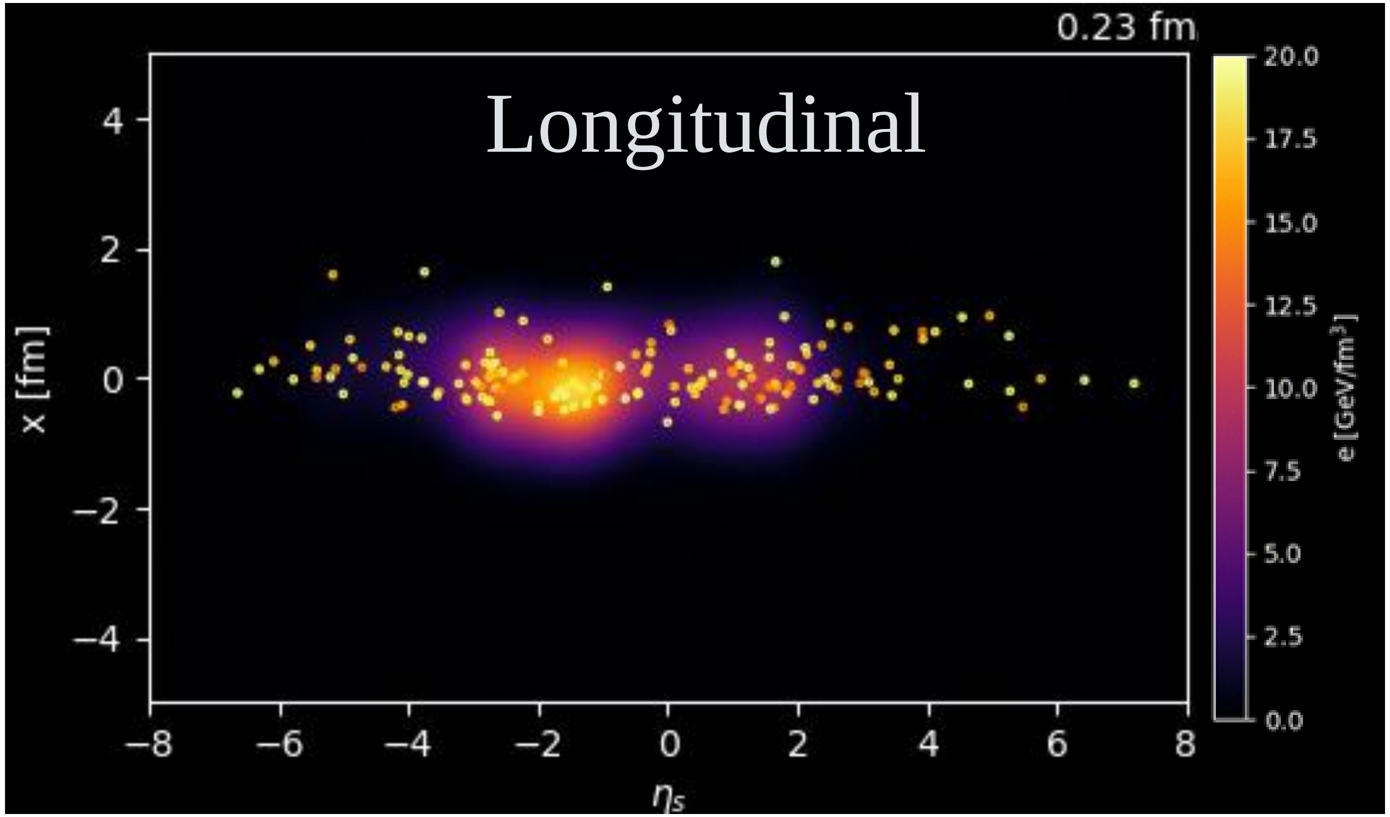

Describes the entire evolution of nuclear collisions

→ SF that reflects collision dynamics

Space-Time Evolution by DCCI2

High-multiplicity p+p collisions at $\sqrt{s} = 7$ TeV

Movies provided by Y. Kanakubo

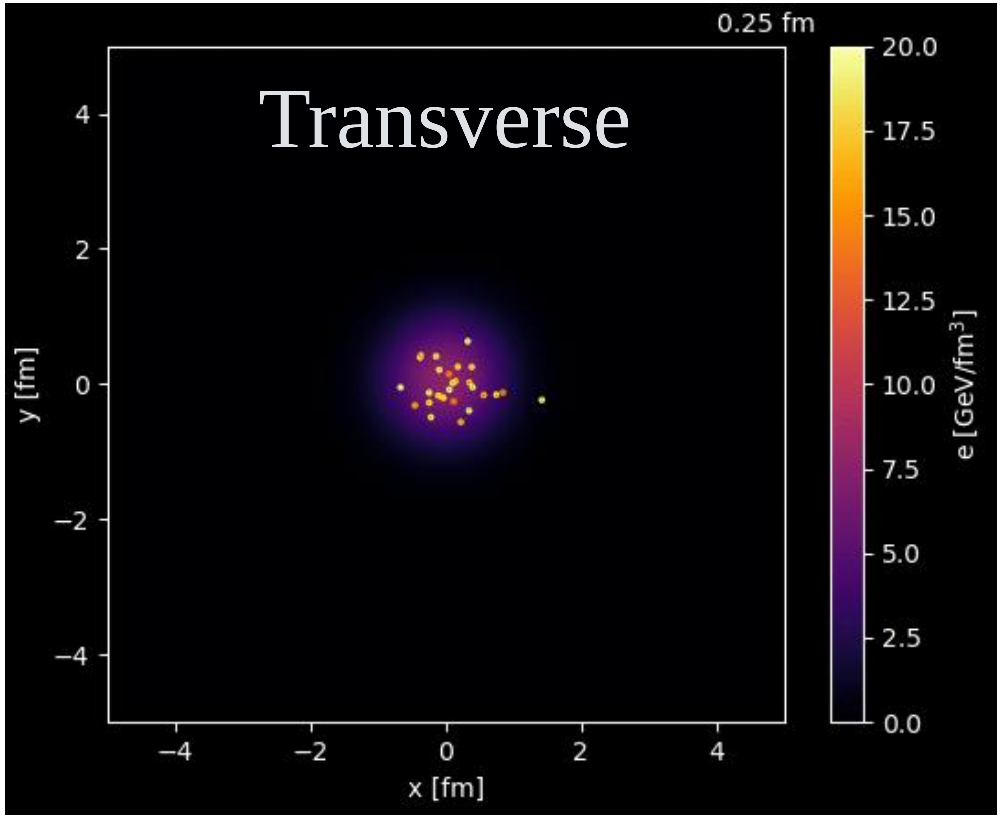

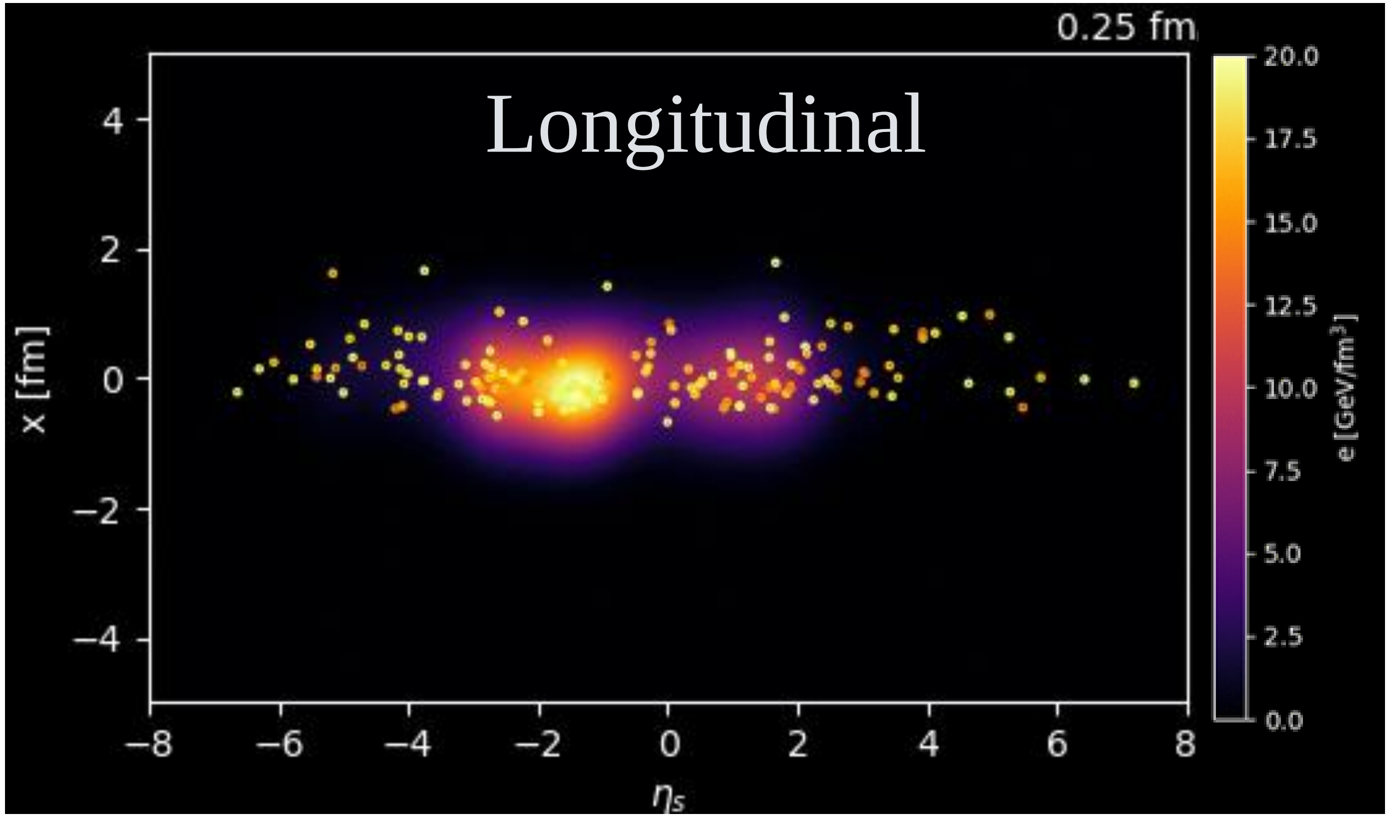

Describes the entire evolution of nuclear collisions

→ SF that reflects collision dynamics

Space-Time Evolution by DCCI2

High-multiplicity p+p collisions at $\sqrt{s} = 7$ TeV

Movies provided by Y. Kanakubo

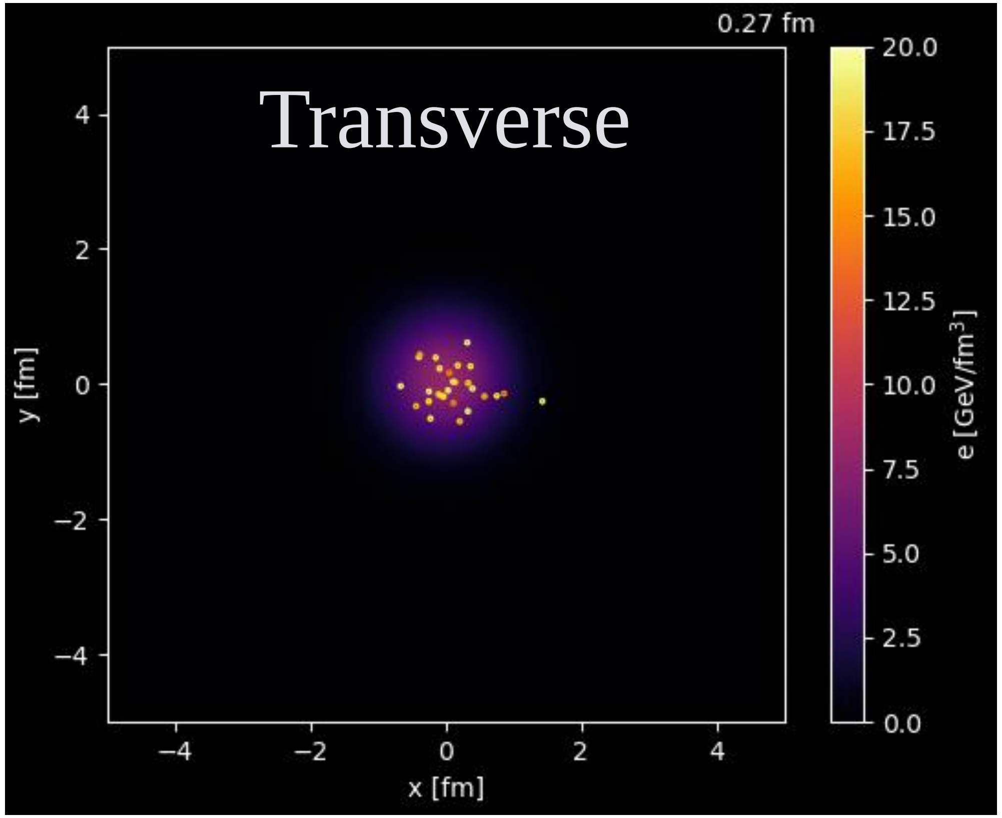

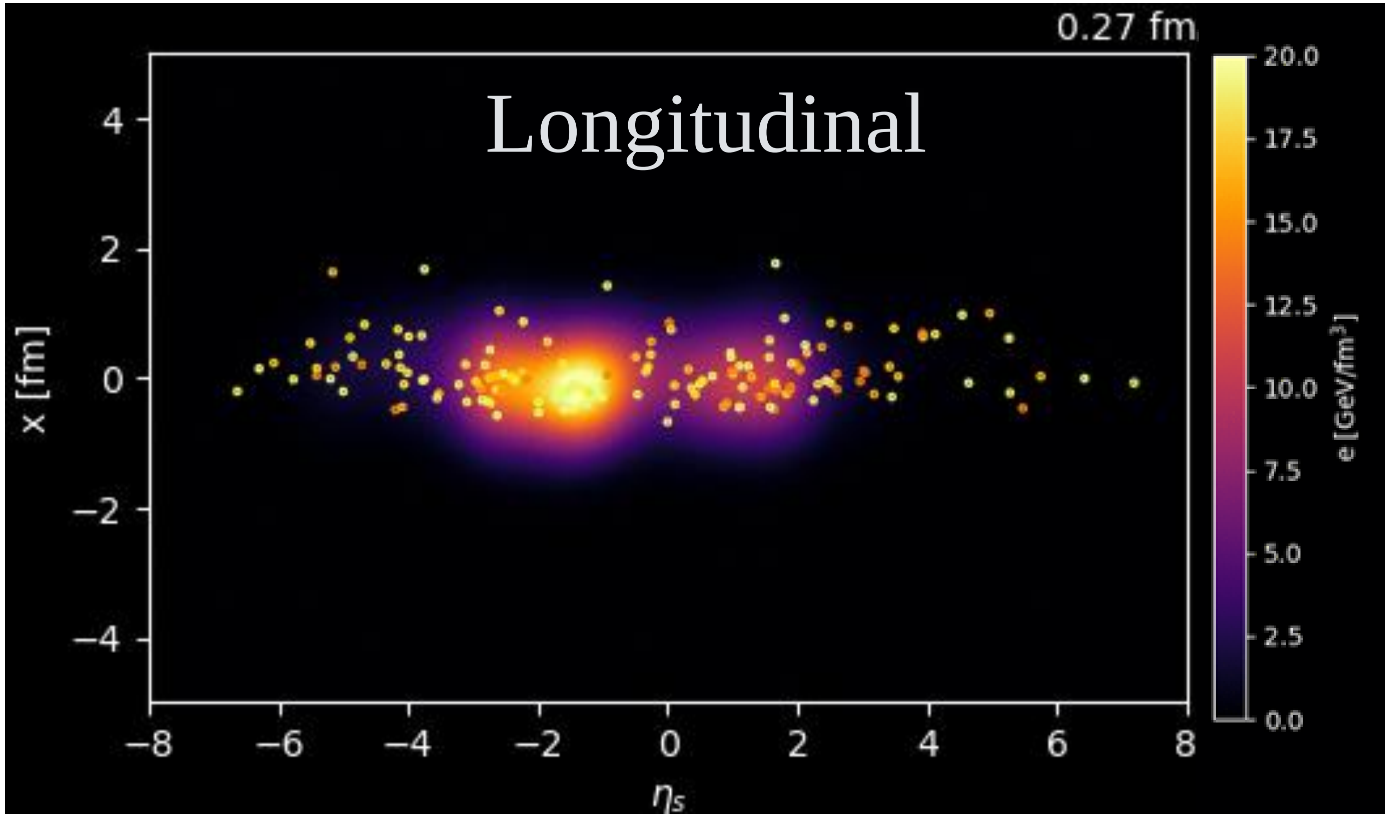

Describes the entire evolution of nuclear collisions

→ SF that reflects collision dynamics

Space-Time Evolution by DCCI2

High-multiplicity p+p collisions at $\sqrt{s} = 7$ TeV

Movies provided by Y. Kanakubo

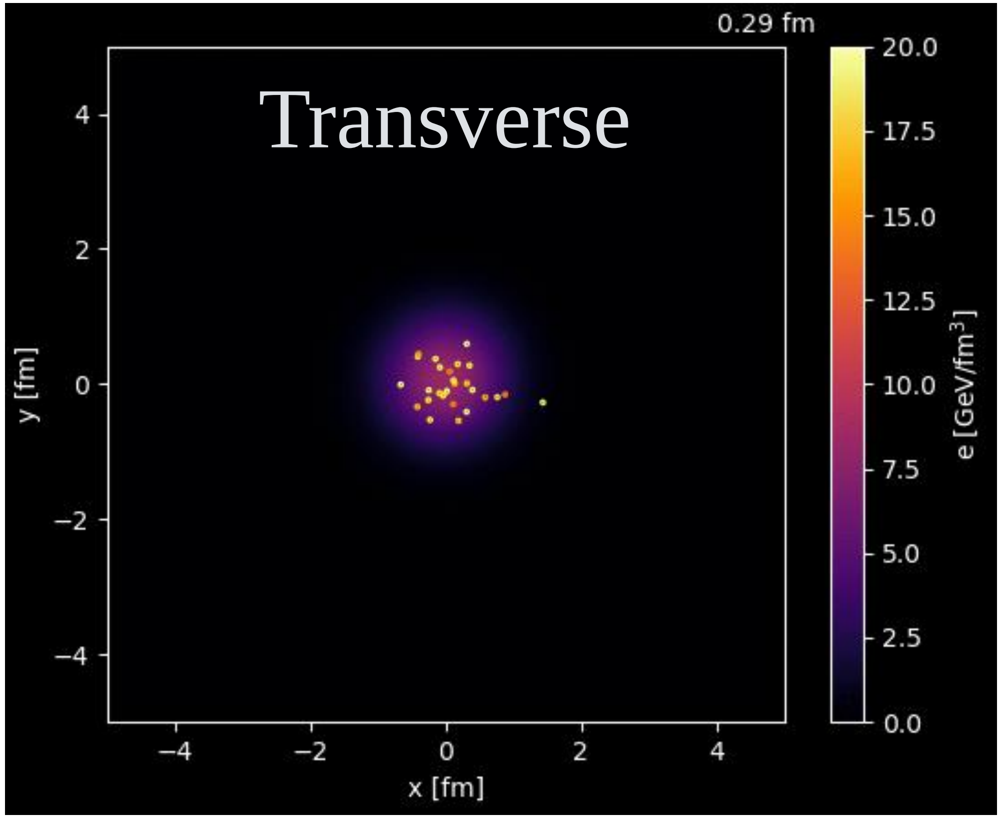

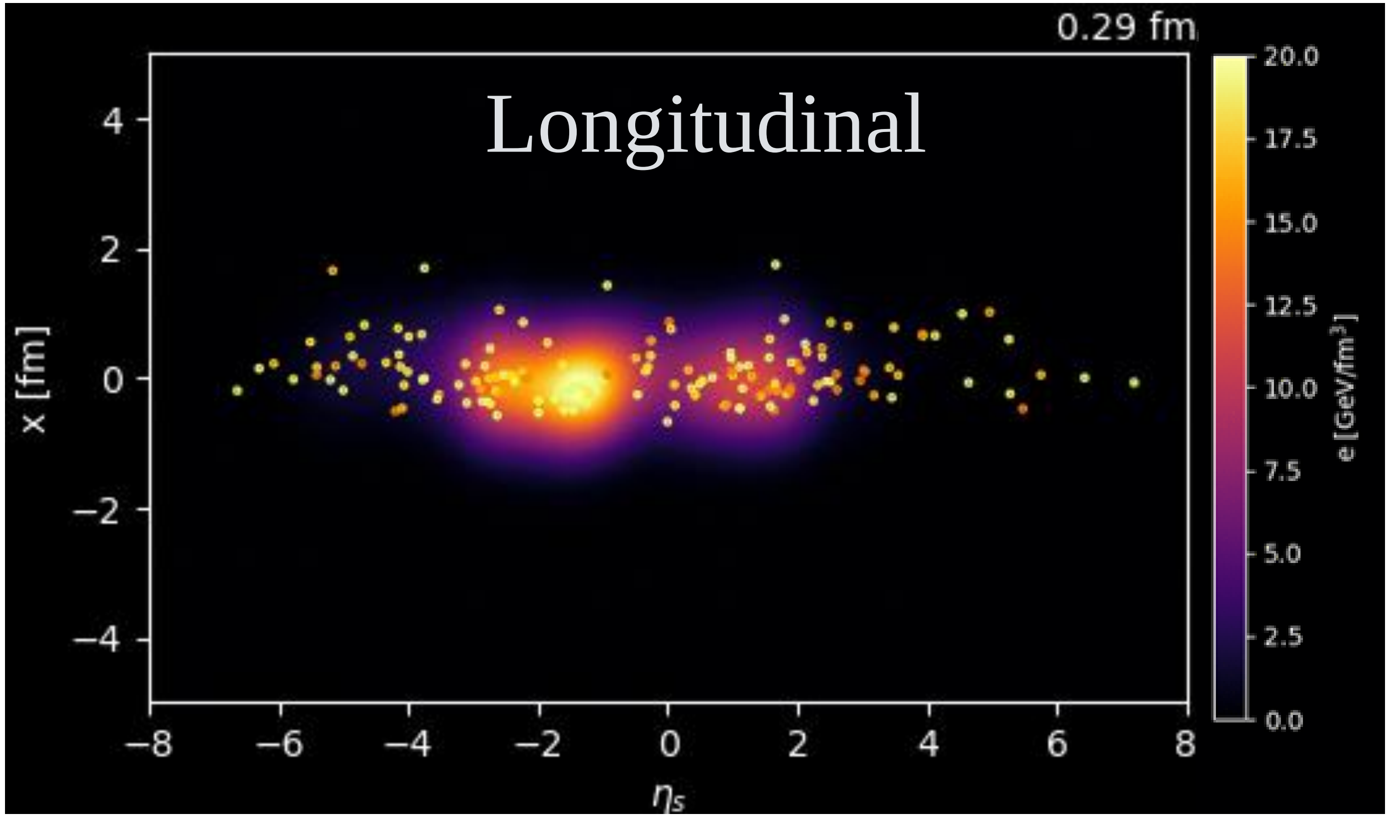

Describes the entire evolution of nuclear collisions

→ SF that reflects collision dynamics

Source Function

High-multiplicity 0-0.17% p+p collisions at $\sqrt{s} = 13$ TeV

Plot: **DCCI2 SF**, Line: Gaussian SF $S(r) \propto \exp(-r^2/4r_0^2)$ w/ $r_0 = 1.08$ fm

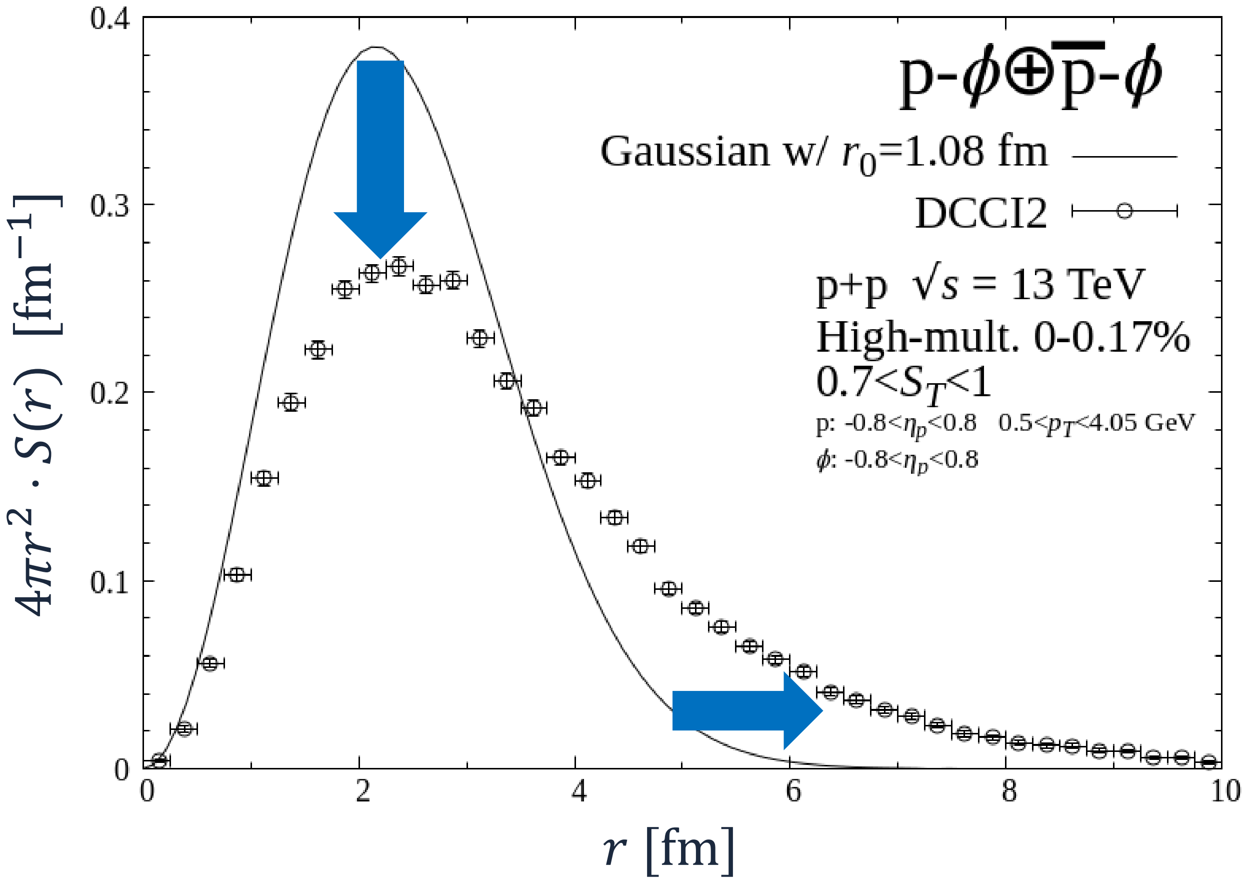

Non-Gaussian long-tail

→ Larger source size $\langle r^2 \rangle$

Mainly due to p rescatterings with surrounding pion gas
“**Pion wind**”

Hadronic rescatterings even in p+p collisions

Correlation Function

Green: $C^{(3/2)}$, Blue: $C^{(1/2)}$, Red: $C^{\mathrm{tot}} = \frac{2}{3}C^{(3/2)} + \frac{1}{3}C^{(1/2)}$

Plots: **DCCI2 SF**, Lines: Gaussian SF w/ $r_0 = 1.08$ fm

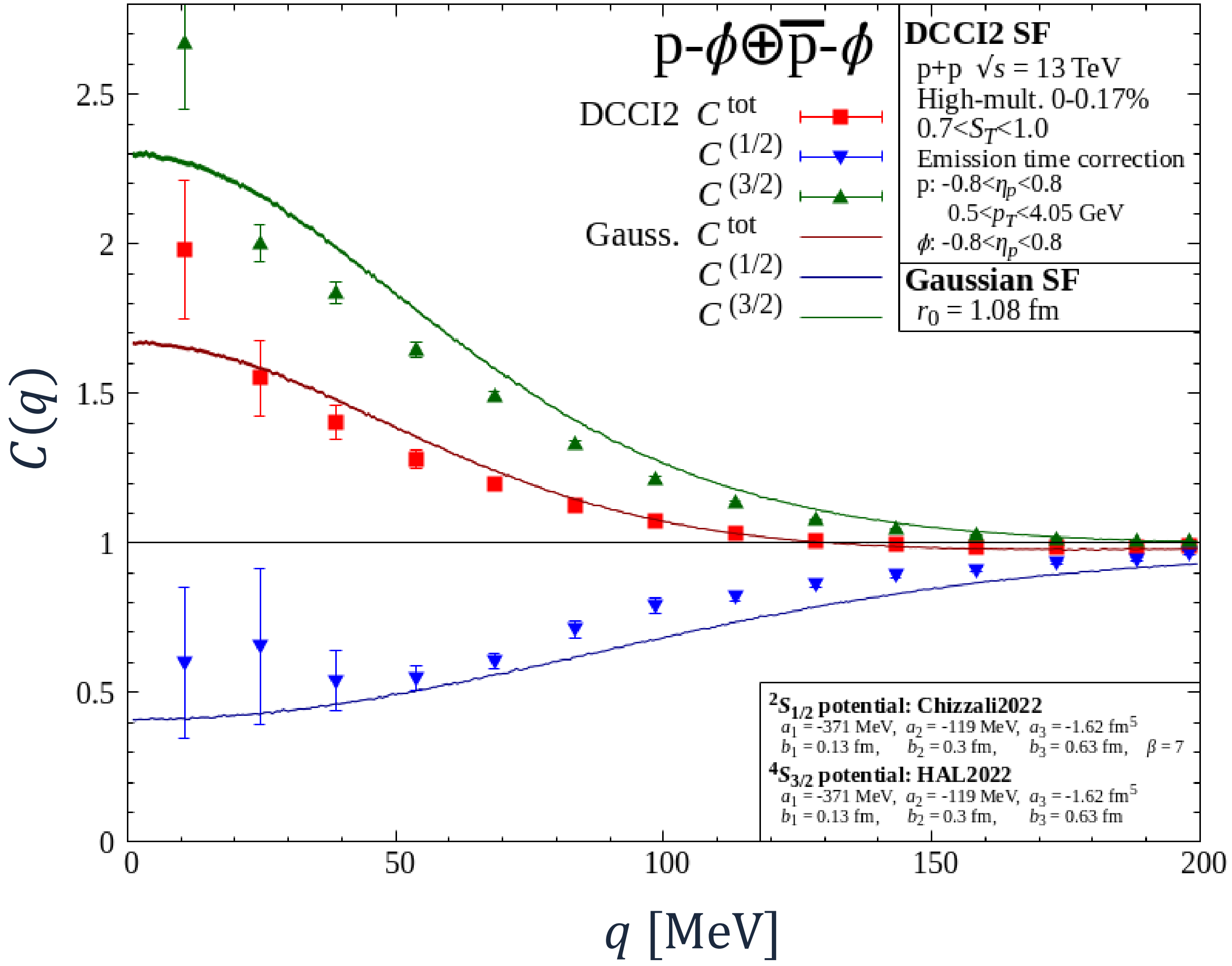

DCCI2 vs. Gaussian

- **Slightly weaker correlation**
  Due to non-Gaussian long-tail
- **Non-trivial behavior at small *q***

A small but statistically significant difference

Correlation Function

Green: $C^{(3/2)}$, Blue: $C^{(1/2)}$, Red: $C^{\mathrm{tot}} = \frac{2}{3}C^{(3/2)} + \frac{1}{3}C^{(1/2)}$

Plots: **DCCI2 SF**, Lines: Gaussian SF w/ $r_0 = 1.08$ fm

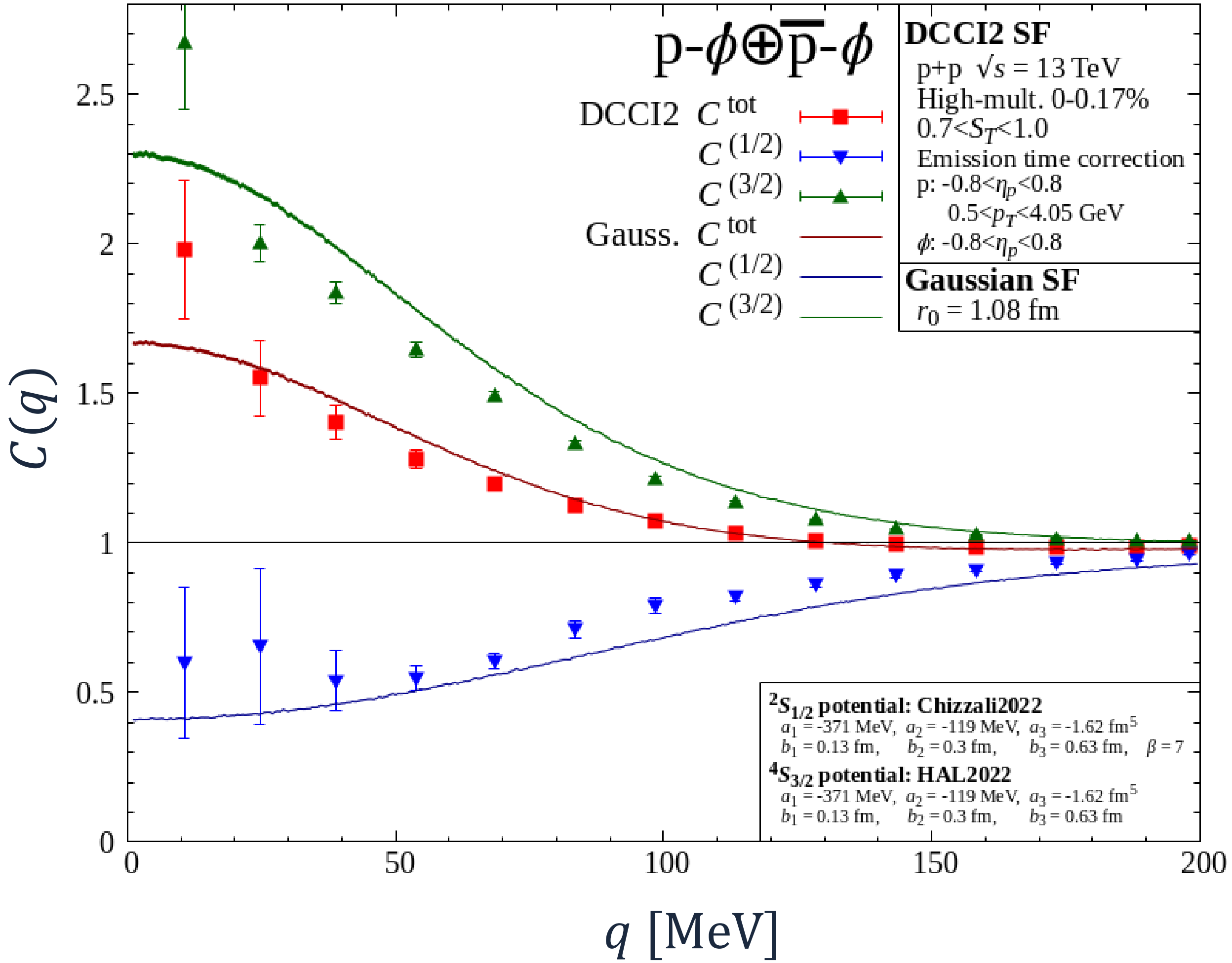

DCCI2 vs. Gaussian

- **Slightly weaker correlation**
  Due to non-Gaussian long-tail
- **Non-trivial behavior at small q**

A small but statistically significant difference

From comparison w/ ALICE data

ALICE, PRL **127**, 172301 (2021)

Indication of a bound state in $^2S_{1/2}$

($E_B \cong$ 10–70 MeV)

Effects of Collectivity

SF generally depends on *q* due to e.g., collectivity

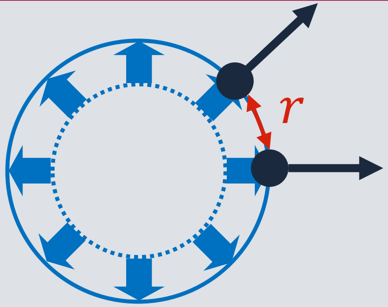

Close in position space
⇕
Close in momentum space

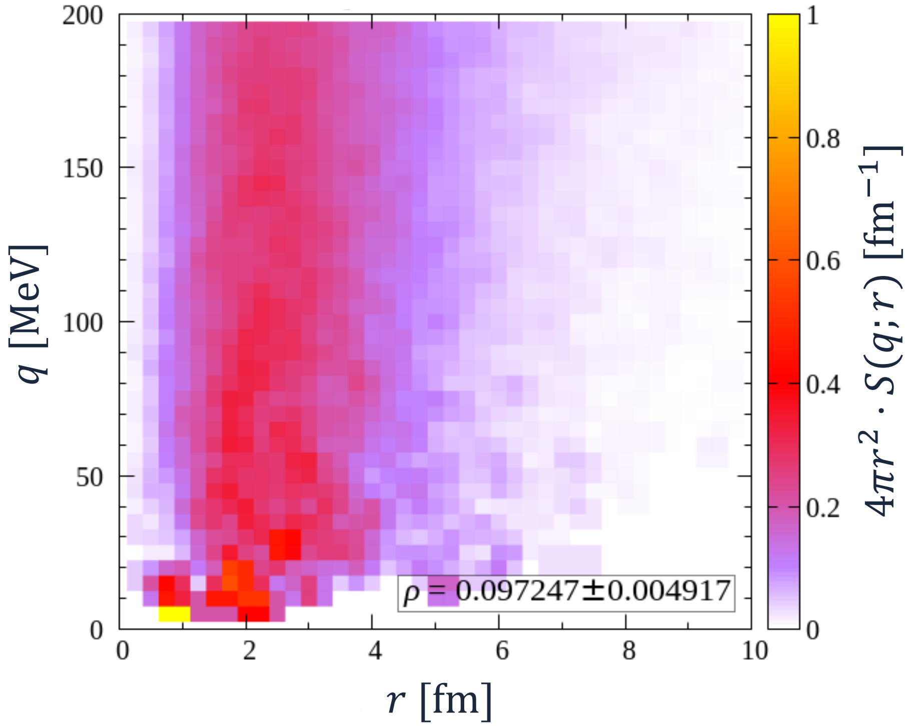

- Slightly positive q–r correlation
- Significant small source at small q

Effects of Collectivity

SF generally depends on q due to e.g., collectivity

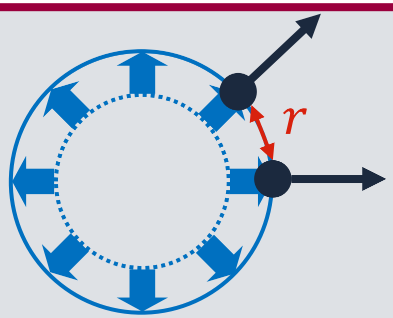

Close in position space
⇳
Close in momentum space

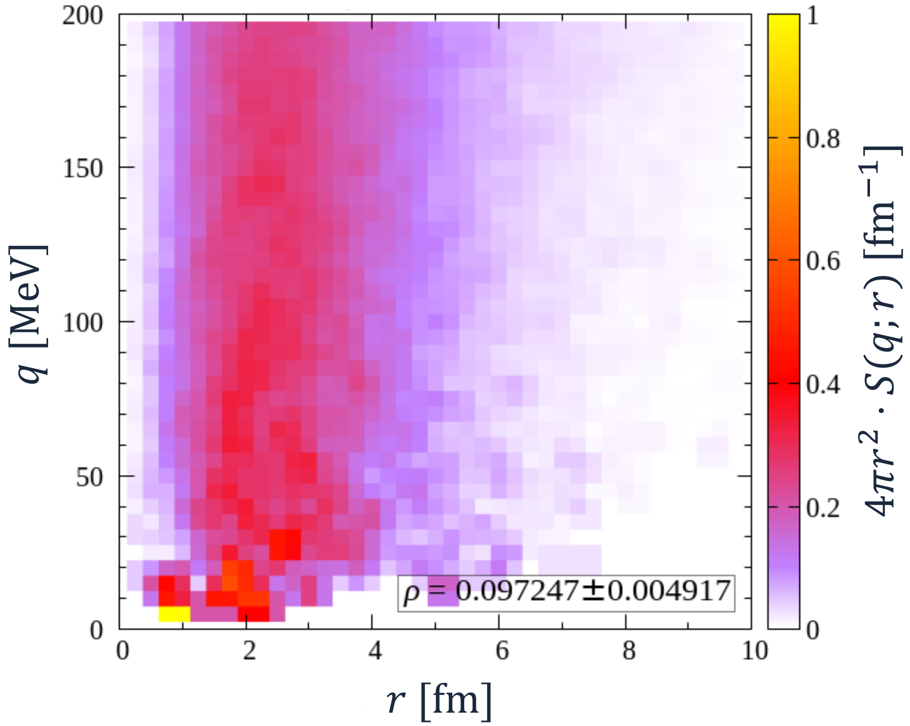

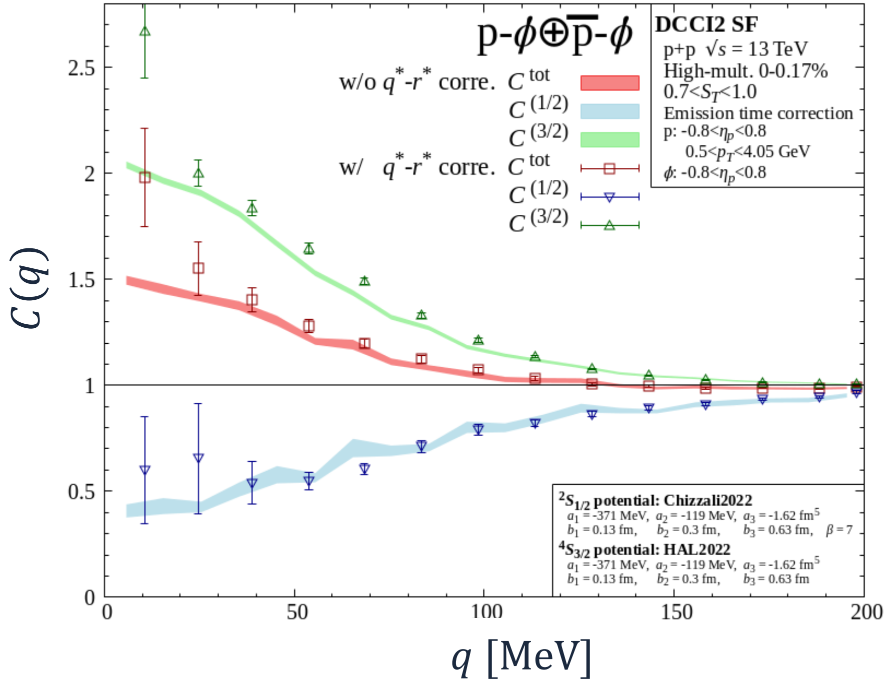

<u>Plots</u>:
W/ q–r correlation

<u>Bands</u>:
W/o q–r correlation

- Slightly positive q–r correlation
- Significant small source at small q

⇨

CF at small q is sensitive to the WF in the scattering region

Effects of Hadronic Afterburner

Primordial core

Direct p and ϕ from core at **hypersurface**

→ **+ Decay** → **Core w/ decay**

→ **+ Decay + Rescatterings** + Corona → **Full** (Comparable to experiment)

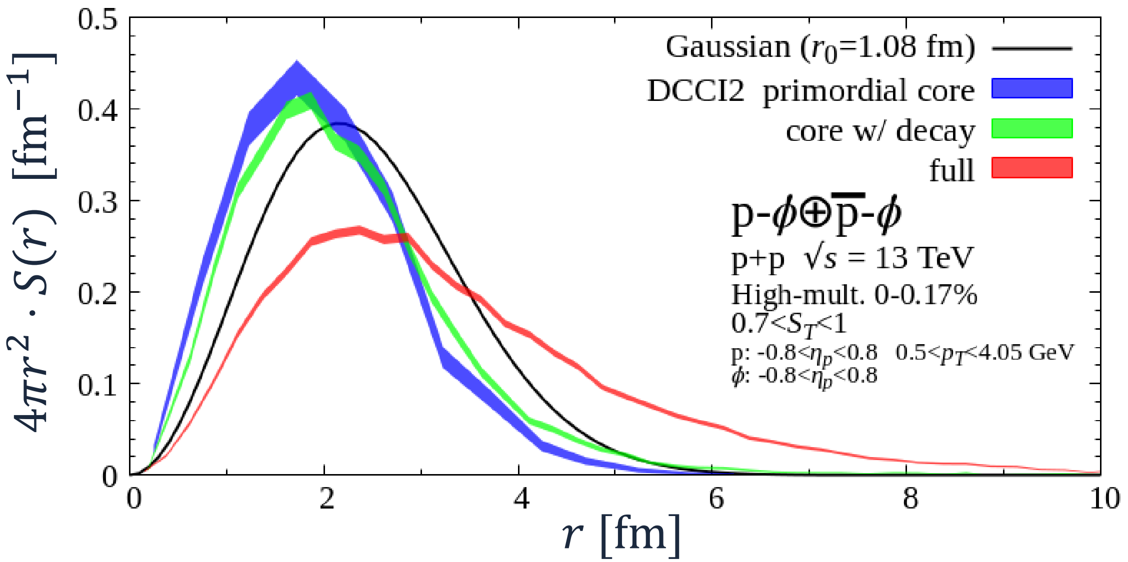

- Distribution at hypersurface ~ Gaussian
- Resonance decay → **A little long-tail**
- Hadronic rescatterings
  → **Long-tail and larger source size**

Effects of Hadronic Afterburner

Primordial core
Direct p and ϕ from core at **hypersurface**

→ **+ Decay** → **Core w/ decay**

→ **+ Decay + Rescatterings** + Corona → **Full** (Comparable to experiment)

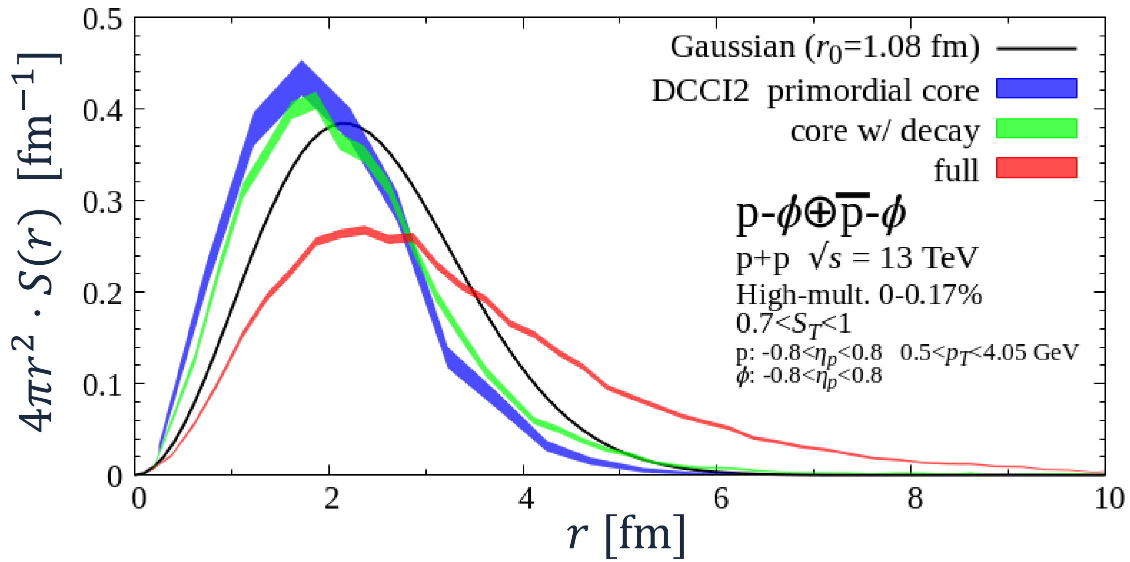

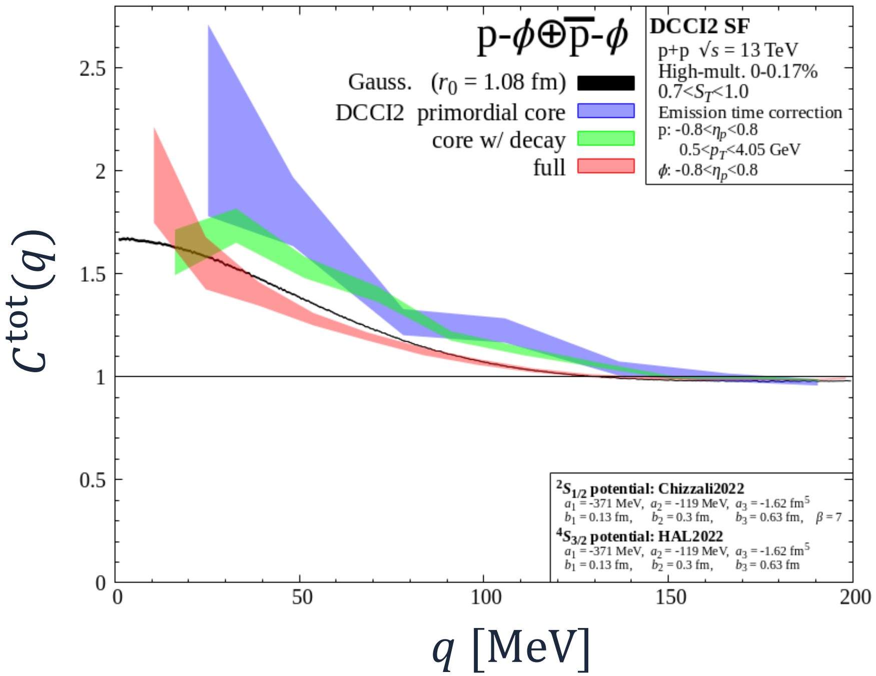

- Distribution at hypersurface ~ Gaussian
- Resonance decay → **A little long-tail**
- Hadronic rescatterings
  → **Long-tail and larger source size**

Larger effects of hadronic rescatterings than resonance decay on SF & CF

Effects of Dynamical Hadron Emission

Emission time difference of the pair from a dynamical model ⇒ **Emission Time Correction (ETC)**

Plots: w/ ETC,   Bands: w/o ETC

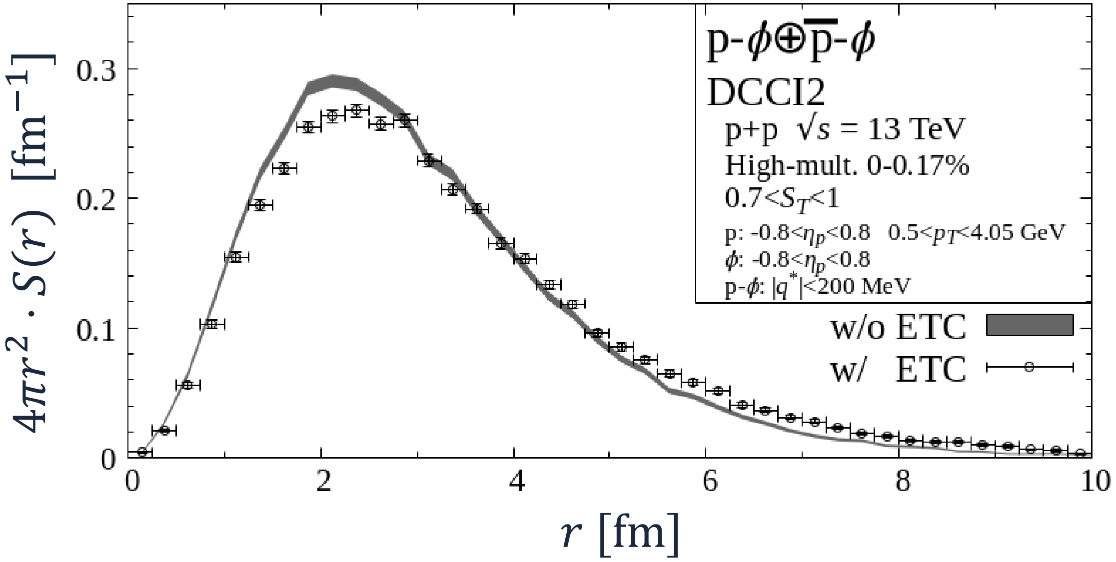

ETC slightly enlarges source size

Effects of Dynamical Hadron Emission

Emission time difference of the pair from a dynamical model ⇒ **Emission Time Correction (ETC)**

Plots: w/ ETC, Bands: w/o ETC

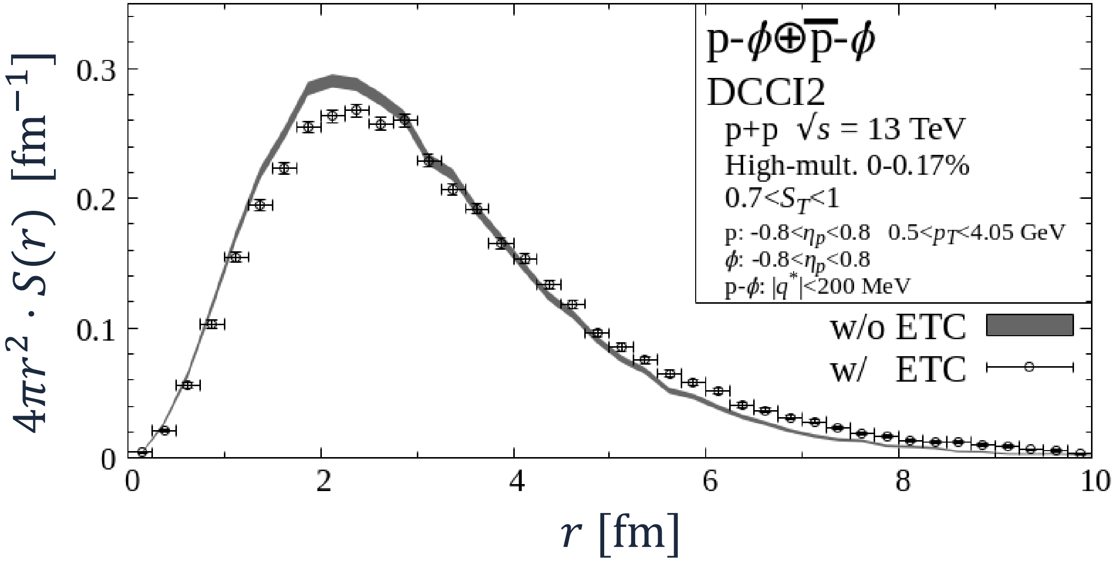

ETC slightly enlarges source size

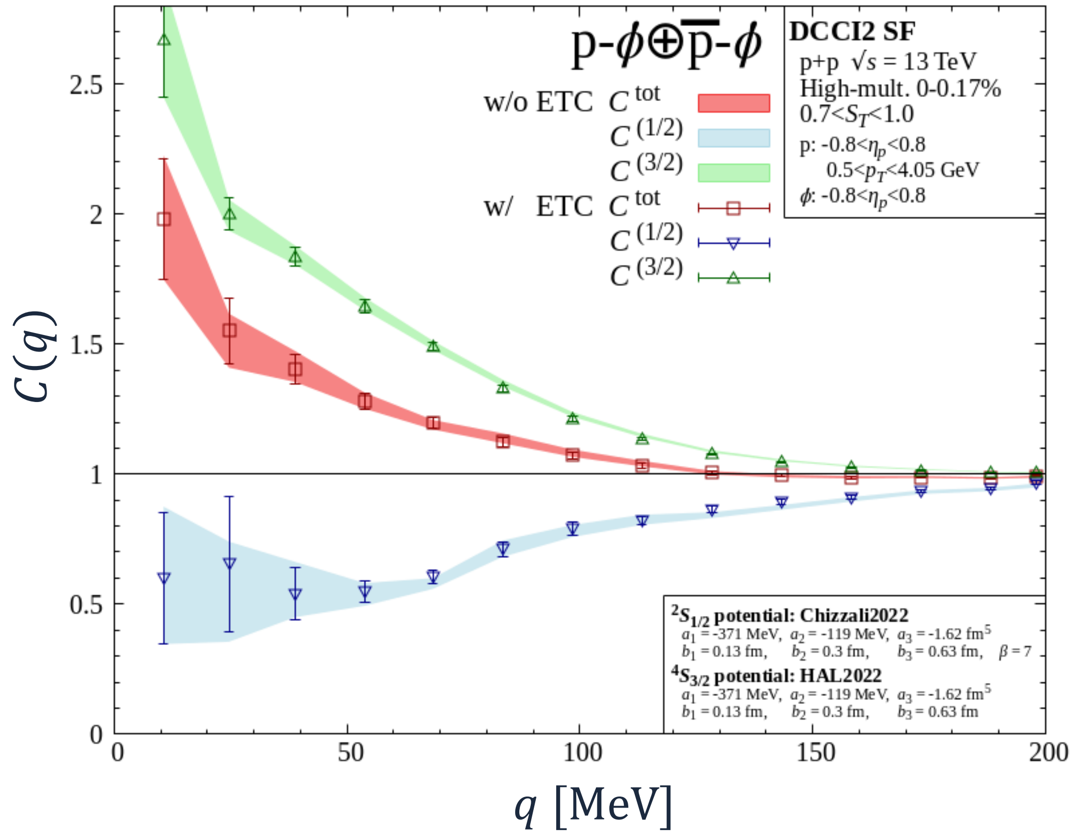

No statistically significant effects on CF in this particular case

Summary

pϕ femtoscopy using SF from a dynamical model (DCCI2)

Effects of collision dynamics

Small but statistically significant

- ✓ Slightly larger source size mainly due to **hadronic rescatterings**
- ✓ SF depends on relative momentum due to e.g., **collectivity**

Phenomenological constraint on interaction

- ✓ Indication of a bound state in $^2S_{1/2}$ channel ($E_B \cong 10$–70 MeV)

Slightly different but qualitatively consistent w/ that using Gaussian SF

Importance of using SF that reflects collision dynamics
for precise studies of hadron interactions via femtoscopy

Backup

Koonin-Pratt Formula

S. E. Koonin, PLB **70**, 43 (1977); S. Pratt, PRL **53**, 1219 (1984)

Assumptions

- **Chaotic source** ~ thermal equilibrium
- Same time approximation
- On-shell approximation
- **Closed system after emission** ~ in vacuum propagation

$$C(\boldsymbol{q},\boldsymbol{P}) = \frac{\int d^4x_a d^4x_b\, S_a(\boldsymbol{p}_a;x_a) S_b(\boldsymbol{p}_b;x_b) |\varphi(\boldsymbol{q};\boldsymbol{r})|^2}{\int d^4x_a\, S_a(\boldsymbol{p}_a;x_a) \int d^4x_b\, S_b(\boldsymbol{p}_b;x_b)}$$

Pair Rest Frame ($\boldsymbol{P} = 0$)

Integrate out CM

$$C(\boldsymbol{q}) = \int d^3r\ S(\boldsymbol{q};\boldsymbol{r})\ |\varphi(\boldsymbol{q};\boldsymbol{r})|^2$$

Rewriting Koonin-Pratt Formula

Spherical SF
$S(q;r)$

Only *s*-wave scattering

$$\varphi(\boldsymbol{q};\boldsymbol{r}) = \exp(i\boldsymbol{q}\cdot\boldsymbol{r}) - j_0(qr) + \varphi_0(q;r)$$

Plane-wave | **Plane-wave (*s*-wave)** | **WF (*s*-wave)**

$$C(\boldsymbol{q}) = \int d^3r\, S(\boldsymbol{q};\boldsymbol{r})\, |\varphi(\boldsymbol{q};\boldsymbol{r})|^2$$

$$= 1 + \int_0^\infty dr\, 4\pi r^2 S(q;r)\, [|\varphi_0(q;r)|^2 - |j_0(qr)|^2]$$

SF
w/ Jacobian

***s*-wave Change**
Increase/Decrease of WF by **FSI**

Interpretation of Correlation

Considering only *s*-wave scattering together with spherical SF

$$C(q) = 1 + \int_0^\infty dr\ 4\pi r^2 S(q;r)\ [|\varphi_0(q;r)|^2 - |j_0(qr)|^2]$$

SF
with Jacobian

***s*-wave Change**
Increase/Decrease in WF by interaction

Deviation of $C(q)$ from 1 = **How much SF "picks up" WF change**

Interpretation of Correlation

Considering only *s*-wave scattering together with spherical SF

$$C(q) = 1 + \int_0^\infty dr \; 4\pi r^2 S(q;r) \; [|\varphi_0(q;r)|^2 - |j_0(qr)|^2]$$

SF
with Jacobian

***s*-wave Change**
Increase/Decrease in WF by interaction

Deviation of $C(q)$ from 1 = **How much SF "picks up" WF change**

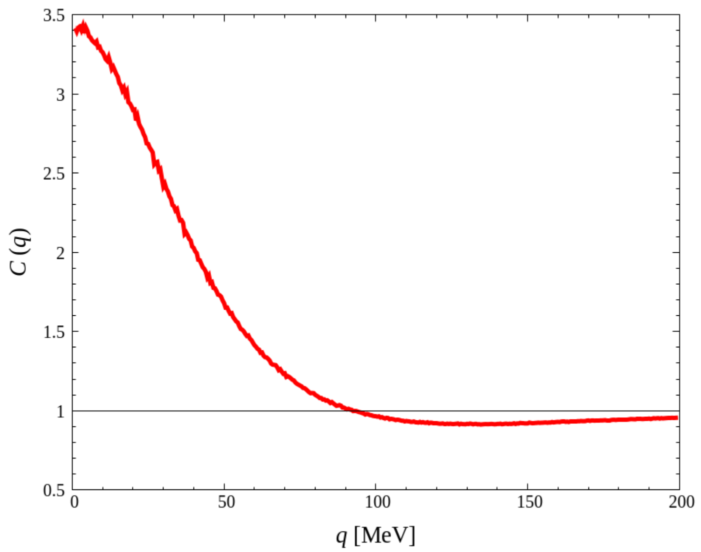

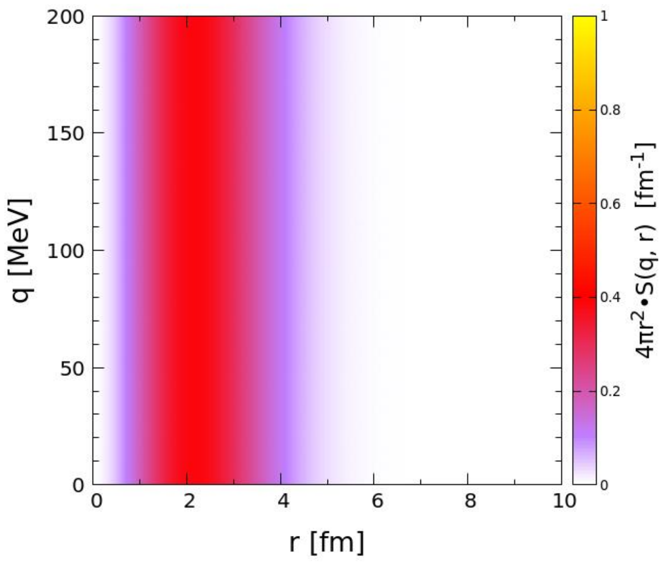

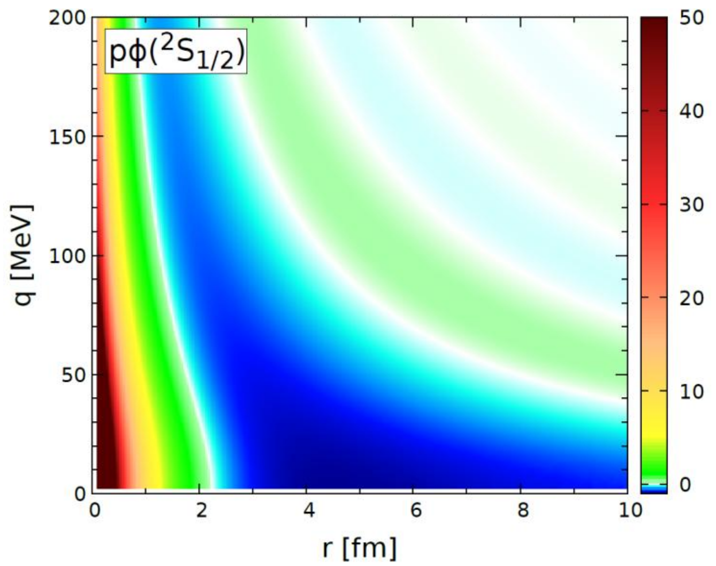

Interpretation of Correlation

Considering only *s*-wave scattering together with spherical SF

$$C(q) = 1 + \int_0^\infty dr \; 4\pi r^2 S(q;r) \; \left[|\varphi_0(q;r)|^2 - |j_0(qr)|^2 \right]$$

SF
with Jacobian

***s*-wave Change**
Increase/Decrease in WF by interaction

Deviation of $C(q)$ from 1 = **How much SF "picks up" WF change**

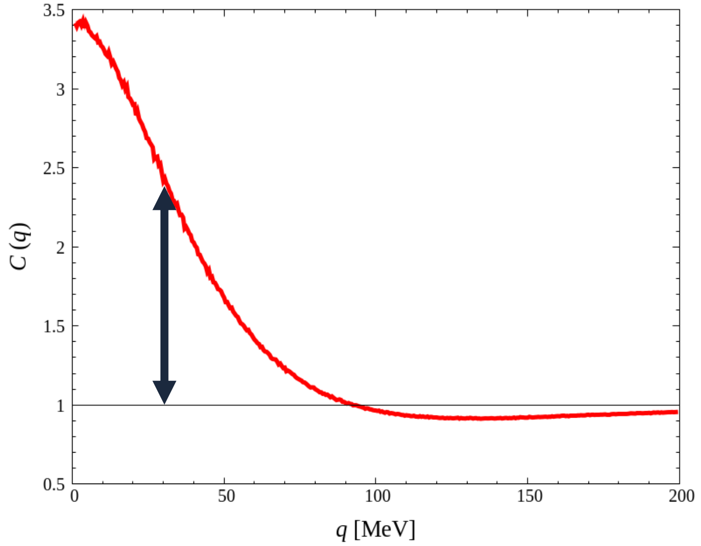

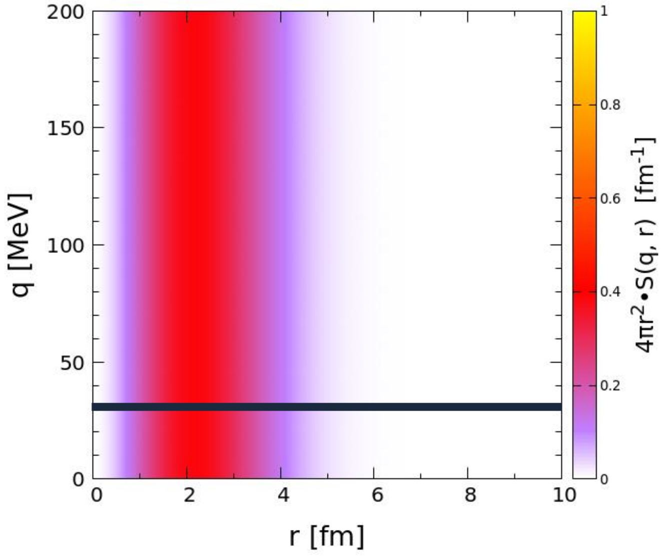

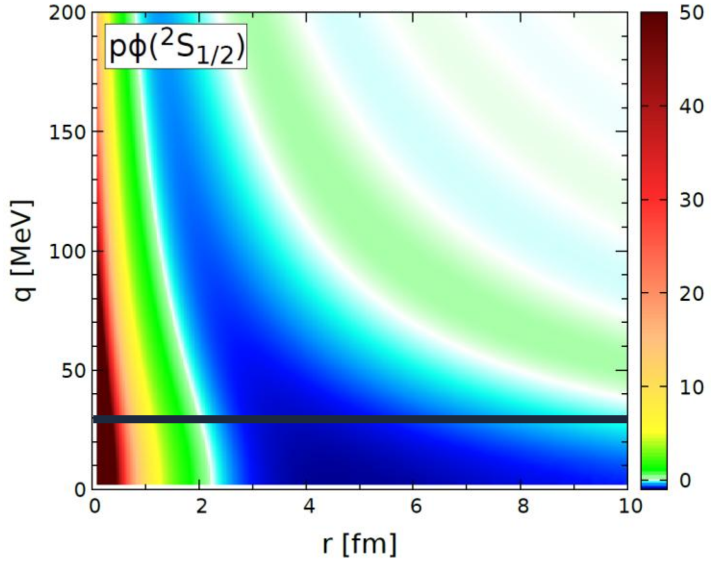

Interpretation of Correlation

Considering only *s*-wave scattering together with spherical SF

$$C(q) = 1 + \int_0^\infty dr \; 4\pi r^2 S(q;r) \; [|\varphi_0(q;r)|^2 - |j_0(qr)|^2]$$

SF
with Jacobian

***s*-wave Change**
Increase/Decrease in WF by interaction

Deviation of $C(q)$ from 1 = **How much SF "picks up" WF change**

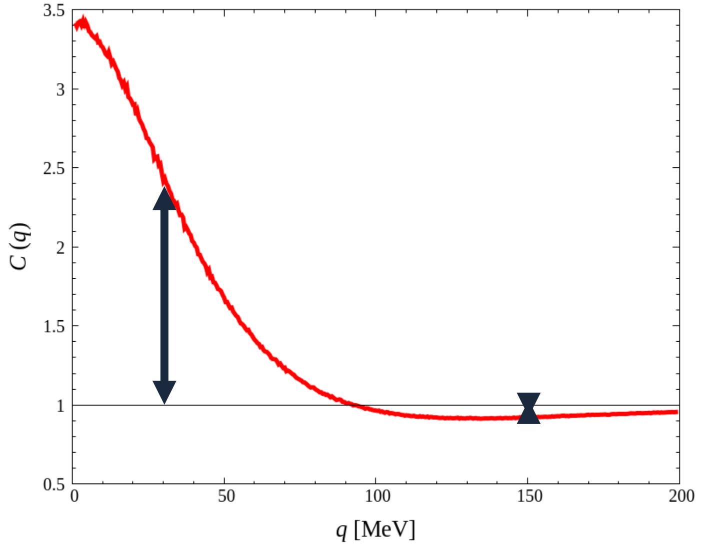

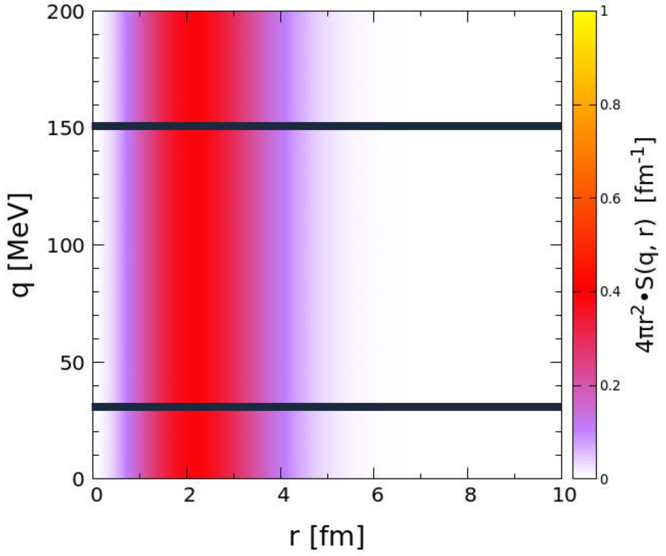

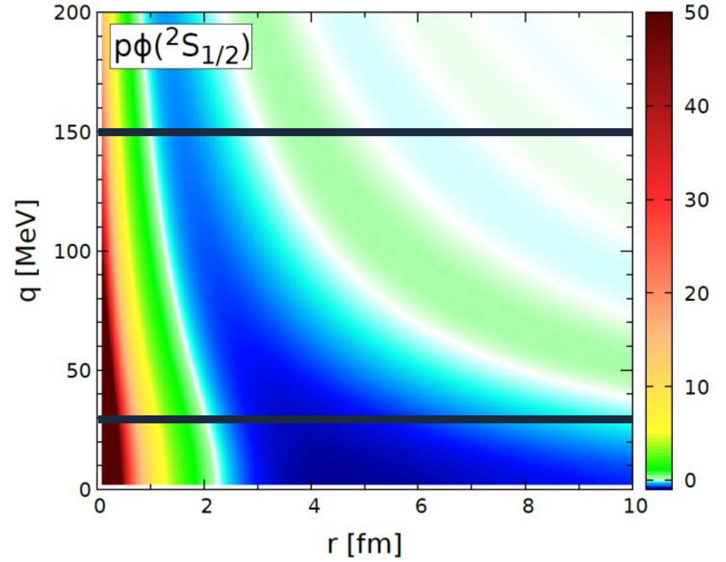

Spin-Average

WF in KP formula = Weighted average of WF in each ${}^{2S+1}L_J$ channel

$$|\varphi|^2 = \sum_{\text{states}(S,L,J)} \omega_{(S,L,J)} \left|\varphi^{(S,L,J)}\right|^2$$

$$\omega_{(S,L,J)} = \frac{2S+1}{(2s_a+1)(2s_b+1)} \frac{2J+1}{(2L+1)(2S+1)}$$

Koonin-Pratt formula

Spin-independent SF ← chaotic source

Spin-averaged CF

$$C^{\text{tot}}(\boldsymbol{q}) = \sum_{\text{states}(S,L,J)} \omega_{(S,L,J)}\, C^{(S,L,J)}(\boldsymbol{q})$$

Comparable w/ exp. CF

WF w/ Final State Interaction

Focusing on low-q region w/ chaotic source and closed system assumptions

→ Steady-state Schrödinger eq. w/ central force

Partial-wave expansion

$$\varphi(\boldsymbol{q};\boldsymbol{r}) = \sum_{l=0}^{\infty}(2l+1)i^l\varphi_l(q;r)P_l(\cos\theta)$$

For each ${}^{2S+1}L_J$ channel,

$$\left[-\frac{1}{2\mu}\frac{d^2}{dr^2}+V(r)+\frac{1}{2\mu}\frac{l(l+1)}{r^2}\right]u_l(q;r) = \frac{q^2}{2\mu}u_l(q;r)$$

$u_l := r\,\varphi_l$

Reduced mass:

$$\mu = \frac{m_a m_b}{m_a + m_b}$$

Lednický-Lyuboshits Model

R. Lednický and V. L. Lyuboshits, Yad. Fiz. **35**, 1316 (1981)

$$C(q) = 1 + \int_0^\infty dr 4\pi r^2 S(q;r)\left[|\varphi_0(q;r)|^2 - |j_0(qr)|^2\right]$$

Assumptions

- **Gaussian SF**: $S(q;r) \approx S(r) \propto \exp\left(-\frac{r^2}{4r_0^2}\right)$
- **Asymptotic WF** (+ effective range correction)

$$C(q) = 1 + \frac{|f_0(q)|^2}{2r_0^2} F_3\left(\frac{r_{\mathrm{eff}}}{r_0}\right) + \frac{2\mathrm{Re}f_0(q)}{\sqrt{\pi}r_0} F_1(2qr_0) - \frac{\mathrm{Im}f_0(q)}{r_0} F_2(2qr_0)$$

$F_1, \ldots, F_3$: Known functions, $f_0(q) = \frac{1}{q\cot\delta_0(q) - iq} \approx \frac{1}{-\frac{1}{a_0} + \frac{1}{2}r_{\mathrm{eff}}q^2 - iq}$

CF becomes a function of a_0, r_{eff}, and r_0

Existing pϕ Femtoscopy 1

Experimental CF ALICE, PRL **127**, 172301 (2021)

High-multiplicity (0–0.17%) **p+p collisions at** $\sqrt{s} = 13$ TeV

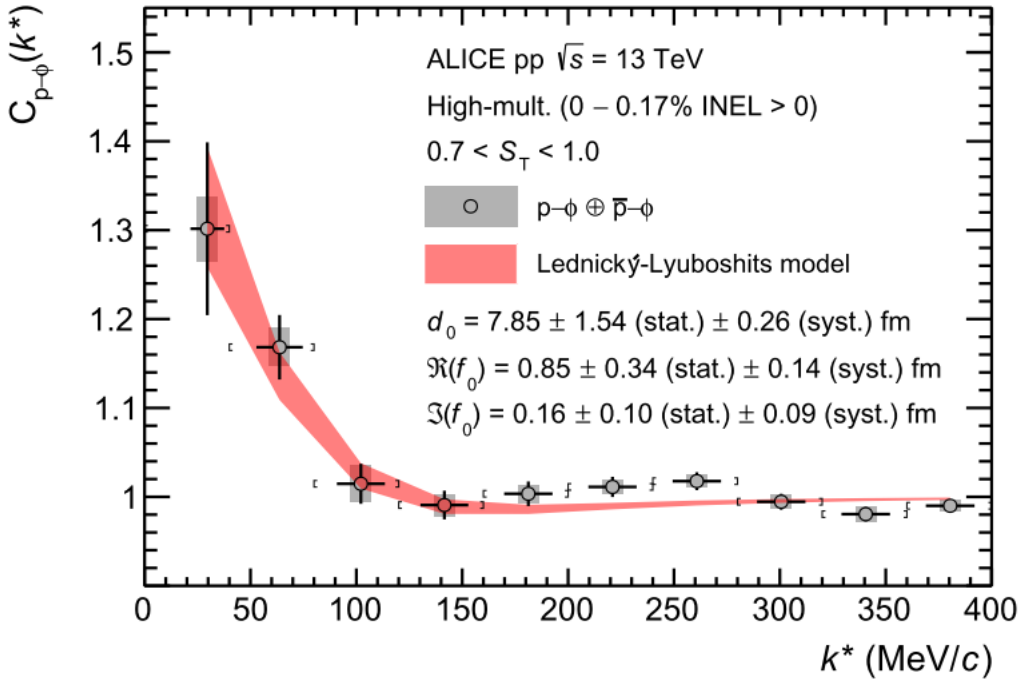

Lednický-Lyuboshits fit

R. Lednický and V. L. Lyuboshits, Yad. Fiz. **35**, 1316 (1981)

Gaussian source size: $r_0 = 1.08$ fm

Scattering length: $a_0 \cong -0.85 - 0.16i$ fm

Effective range: $r_{\text{eff}} \cong 7.85$ fm

Attractive pϕ interaction **as a spin-average**

Existing pϕ Femtoscopy 2

Spin-channel-by-channel femtoscopy

E. Chizzali *et al.*, PLB **848**, 138358 (2023)

Gaussian source size: $r_0 = 1.08$ fm

$^4S_{3/2}$: HAL QCD potential Y. Lyu *et al.*, PRD 106, 074507 (2022)

$a_0^{(3/2)} \cong -1.43$ fm, $r_{\mathrm{eff}}^{(3/2)} \cong 2.36$ fm

Attraction without bound states

$^2S_{1/2}$: **Parametrized potential ← Constrain by experimental CF**

$a_0^{(1/2)} \cong 1.54 - i0.00$ fm, $r_{\mathrm{eff}}^{(1/2)} \cong 0.39 + i0.00$ fm

- **Strong attraction**
- **Small effects of channel-coupling**

Indication of a pϕ bound state

Overview of Present Study

SF should reflect the complex dynamics of nuclear collisions

This study: **Femtoscopy using SF from a dynamical model**

Overview of Present Study

SF should reflect the complex dynamics of nuclear collisions

This study: **Femtoscopy using SF from a dynamical model**

pϕ potential

$^4S_{3/2}$: Lattice QCD $^2S_{1/2}$: **Parametrization**

Schrödinger eq.

WF

Overview of Present Study

SF should reflect the complex dynamics of nuclear collisions

This study: **Femtoscopy using SF from a dynamical model**

pϕ potential

$^4S_{3/2}$: Lattice QCD $^2S_{1/2}$: **Parametrization**

Schrödinger eq.

New

SF from **a dynamical model**

WF

Koonin-Pratt formula

New

pϕ CF from **a dynamical model**

Overview of Present Study

SF should reflect the complex dynamics of nuclear collisions

This study: **Femtoscopy using SF from a dynamical model**

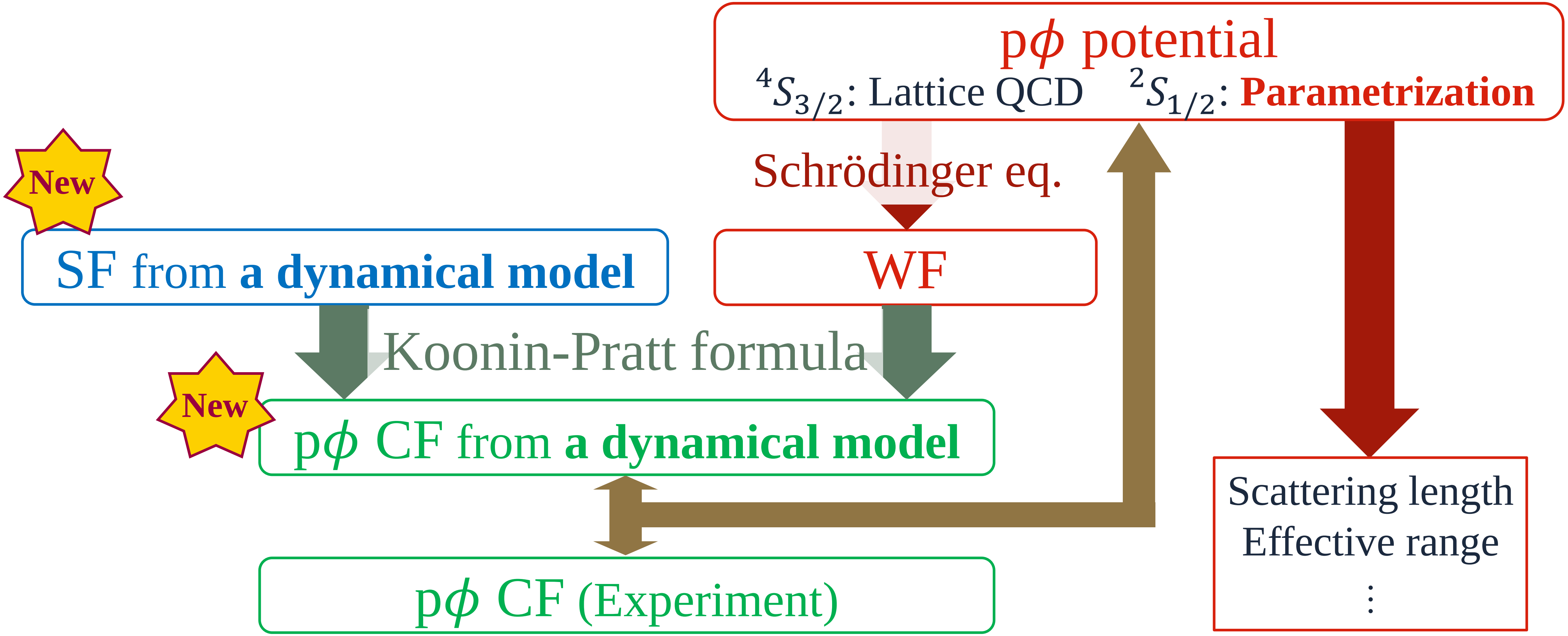

$^4S_{3/2}$ Channel

Argonne-type form factor:

$f(r;b_3) = \left[1 - e^{-(r/b_3)^2}\right]^2$

Parameter	Fitted value
a_1 [MeV]	−371±27
b_1 [fm]	0.13±0.01
a_2 [MeV]	−119±39
b_2 [fm]	0.30±0.05
a_3 [fm^5]	−1.62±0.23
b_3 [fm]	0.63±0.04

HAL QCD potential Y. Lyu *et al.*, PRD **106**, 074507 (2022)

Lattice QCD at nearly physical point ($m_\pi = 146.4$ MeV)

$$V^{(3/2)}(r) = a_1 e^{-(r/b_1)^2} + a_2 e^{-(r/b_2)^2} + a_3 m_\pi^4 f(r;b_3)\frac{e^{-2m_\pi r}}{r^2}$$

Short-range attraction | TPE

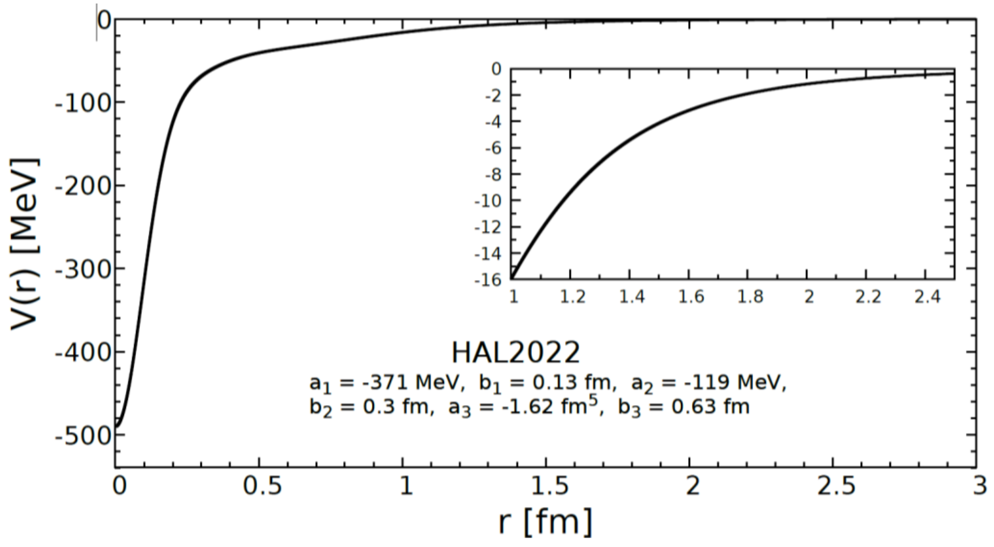

No bound state

WF change: $|\varphi_0|^2 - (j_0)^2$

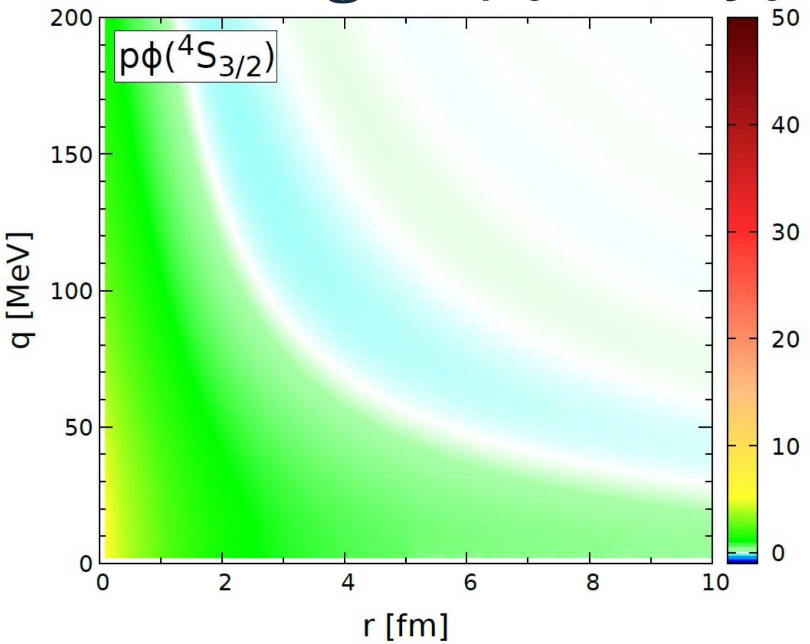

Enhancement at small *qr*

due to attraction

$^2S_{1/2}$ Channel

Parametrized potential

E. Chizzali *et al.*, PLB **848**, 138358 (2023)

Channel-couplings are neglected for simplicity

$$V^{(1/2)}(r) = \beta\left[a_1 e^{-(r/b_1)^2} + a_2 e^{-(r/b_2)^2}\right] + a_3 m_\pi^4 f(r; b_3)\frac{e^{-2m_\pi r}}{r^2}$$

Short-range interaction | TPE

Only one adjustable parameter

β

default: $\beta = 7$

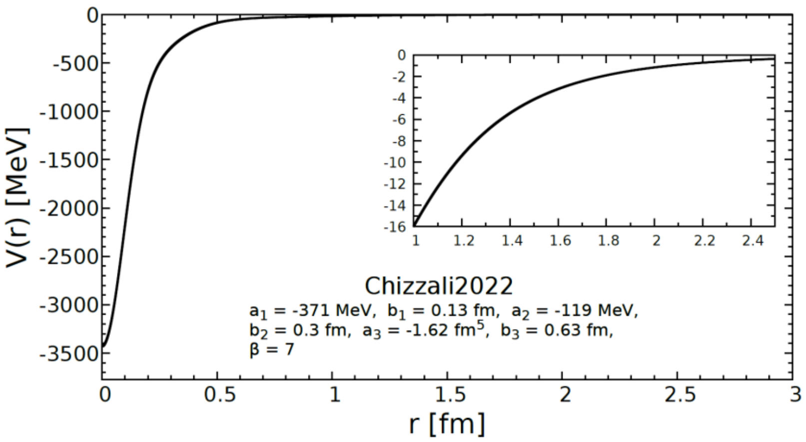

$a_0 = 1.99$ fm

$r_{\text{eff}} = 0.46$ fm

A bound state

WF change: $|\varphi_0|^2 - (j_0)^2$

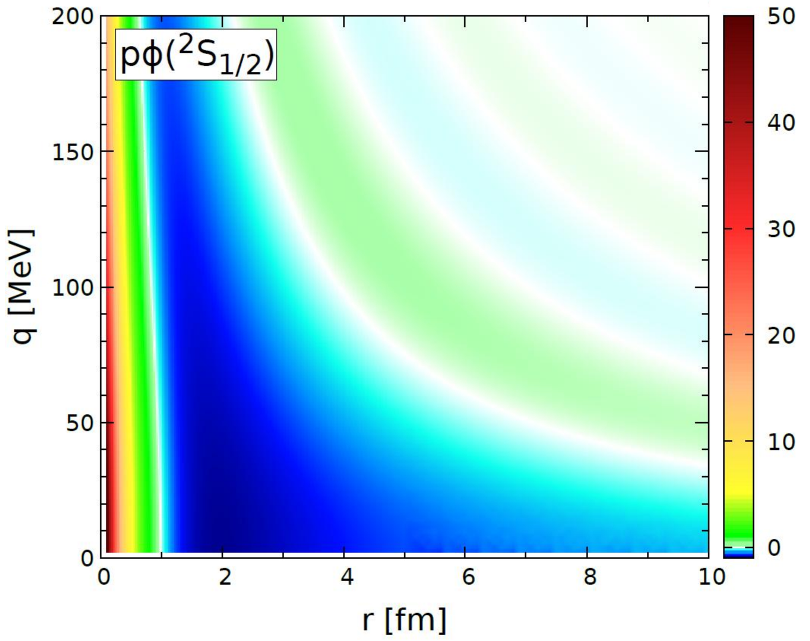

- **Strong enhancement at small qr**
- **“Negative valley” around a_0**

WF Change: Interaction-Dependence

Weak — Attractive potential w/ a bound state — Strong

$\beta = 6$	$\beta = 7$	$\beta = 8$	$\beta = 9$
$a_0 = 4.54$ fm	$a_0 = 1.99$ fm	$a_0 = 1.23$ fm	$a_0 = 0.85$ fm
$E_B = 2.3$ MeV	$E_B = 13.3$ MeV	$E_B = 37.5$ MeV	$E_B = 93.1$ MeV

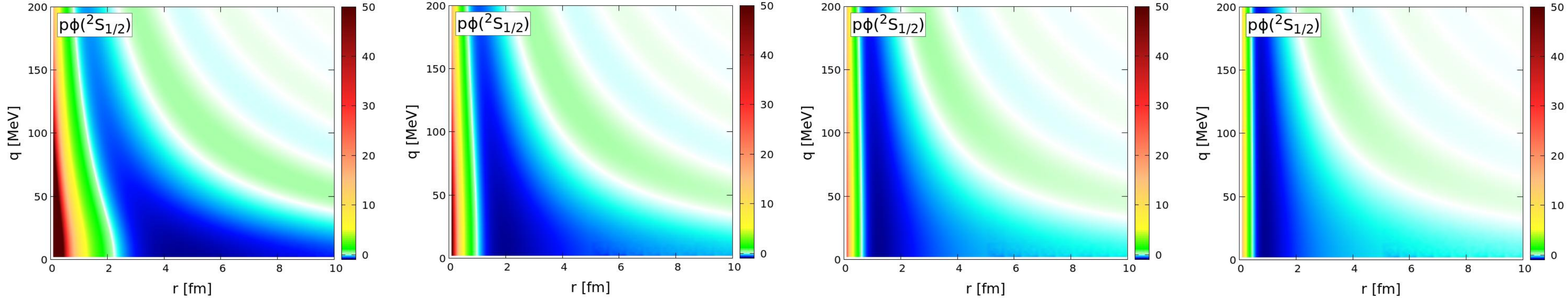

The negative valley moves towards the small *r* region

Compare with ALICE Data

$C^{(3/2)}$: Fixed, $C^{(1/2)}$: Change with β

Compare $C^{\mathrm{tot}} = \frac{2}{3}C^{(3/2)} + \frac{1}{3}C^{(1/2)}$ with ALICE data

$\boldsymbol{\beta = 6}$

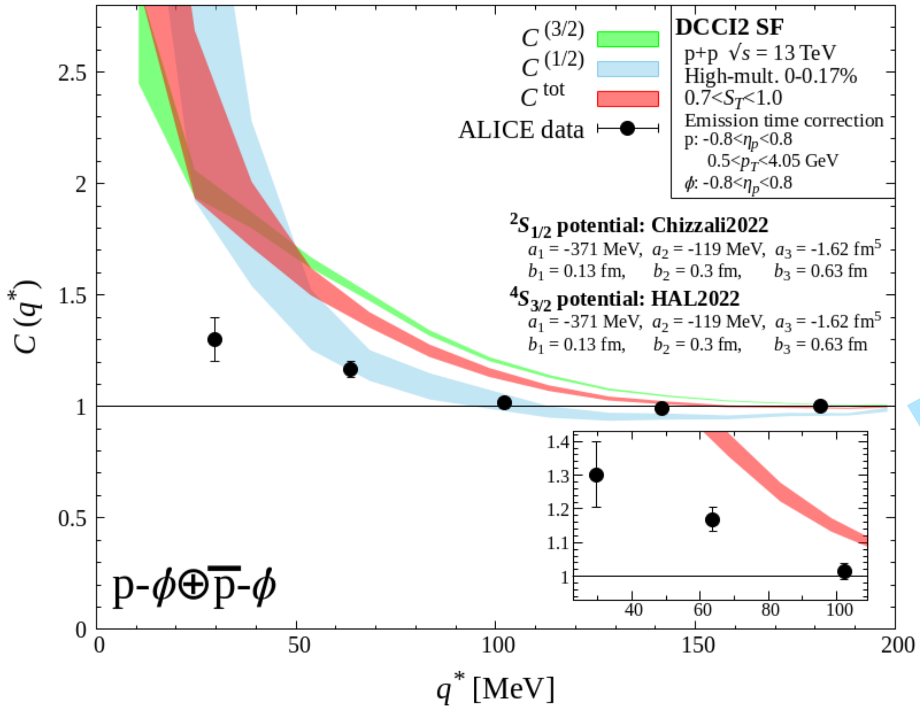

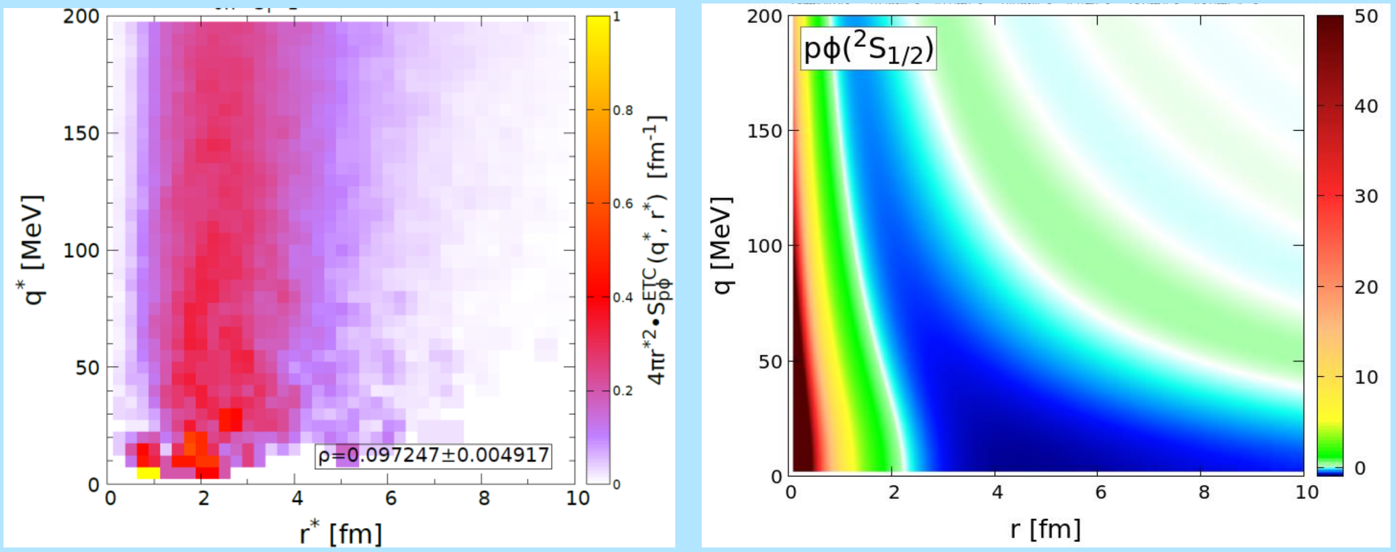

SF picks up strong positive region of WF

$C^{\mathrm{tot}} > C^{\mathrm{exp}}$

Compare with ALICE Data

$C^{(3/2)}$: Fixed, $C^{(1/2)}$: Change with β

Compare $C^{\mathrm{tot}} = \frac{2}{3} C^{(3/2)} + \frac{1}{3} C^{(1/2)}$ with ALICE data

$\boldsymbol{\beta = 9}$

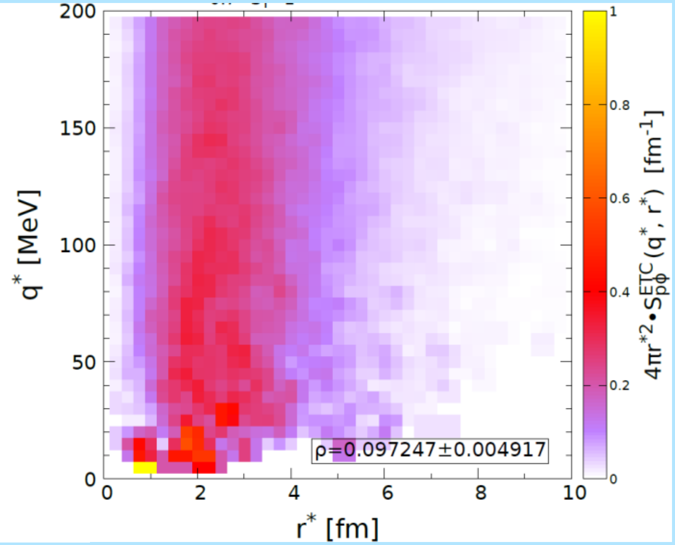

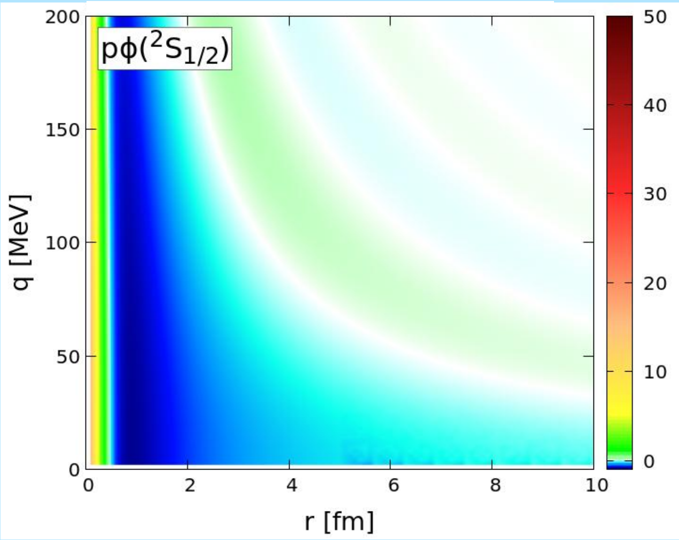

SF cannot pick up negative valley efficiently

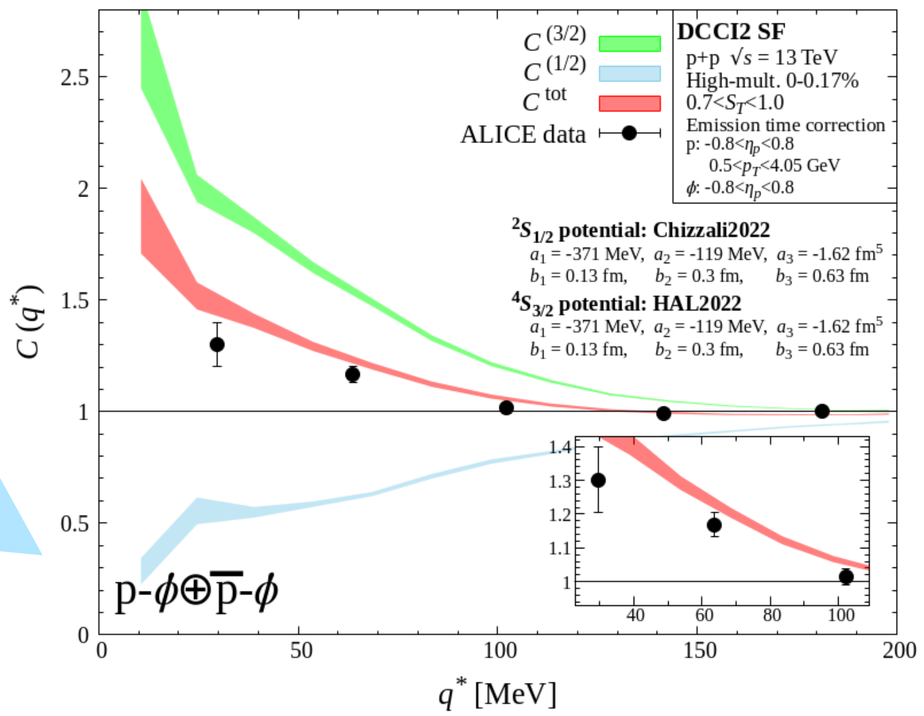

$C^{\mathrm{tot}} > C^{\mathrm{exp}}$

Compare with ALICE Data

$C^{(3/2)}$: Fixed, $C^{(1/2)}$: Change with β

Compare $C^{\text{tot}} = \frac{2}{3}C^{(3/2)} + \frac{1}{3}C^{(1/2)}$ with ALICE data

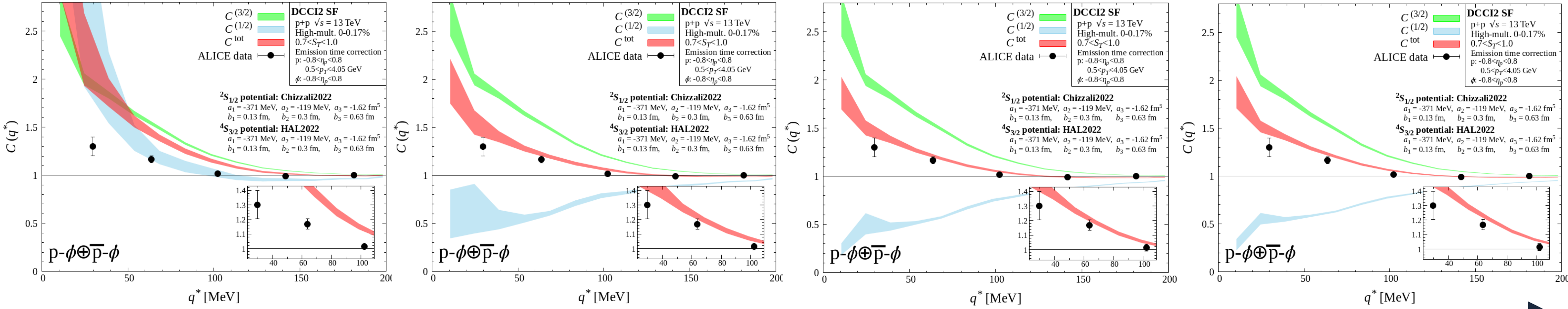

$\boldsymbol{\beta = 6}$

$a_0 = 4.54$ fm

$E_B = 2.3$ MeV

$\boldsymbol{\beta = 7}$

$a_0 = 1.99$ fm

$E_B = 13.3$ MeV

$\boldsymbol{\beta = 8}$

$a_0 = 1.23$ fm

$E_B = 37.5$ MeV

$\boldsymbol{\beta = 9}$

$a_0 = 0.85$ fm

$E_B = 93.1$ MeV

Overestimate | Agree within errors | Overestimate

Emission Time Correction (ETC)

<u>Problem</u>

Dynamical model → **Emission time difference:** $S(\boldsymbol{q}; r^0 \neq 0, \boldsymbol{r})$

Violates **same time approximation** in KP formula

Free propagation until the other's emission

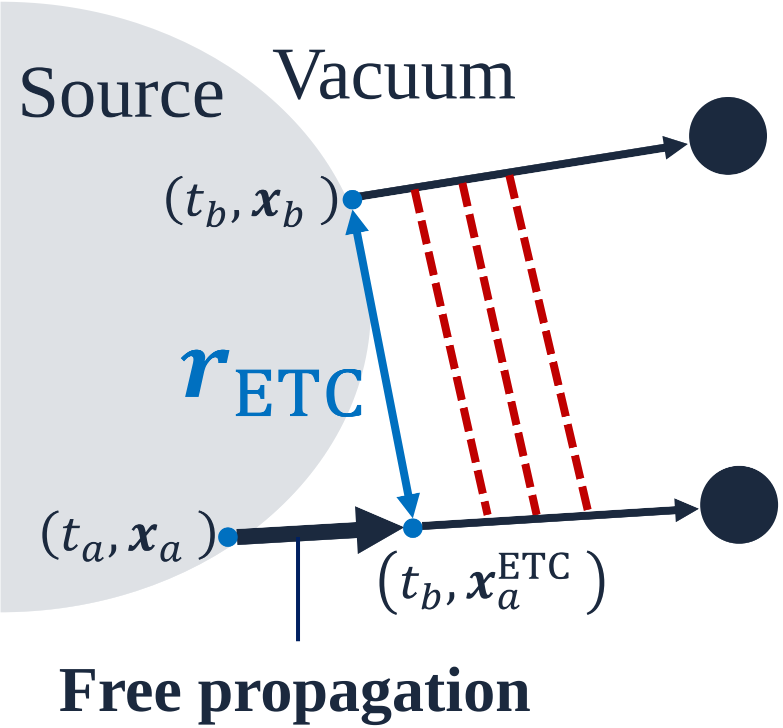

$$S(\boldsymbol{q}; r^0 \neq 0, \boldsymbol{r}) \xrightarrow{\text{ETC}} S^{\mathrm{ETC}}(\boldsymbol{q}; \boldsymbol{r}_{\mathrm{ETC}})\delta(r^0)$$

$$\boldsymbol{r}_{\mathrm{ETC}} = \boldsymbol{r} + \frac{\boldsymbol{p}_a}{E_a}(t_b - t_a)\theta(t_b - t_a) - \frac{\boldsymbol{p}_b}{E_b}(t_a - t_b)\theta(t_a - t_b)$$

Correction

Core–Corona Ratio

Y. Kanakubo, Y. Tachibana, and T. Hirano, PRC **105**, 024905 (2022)

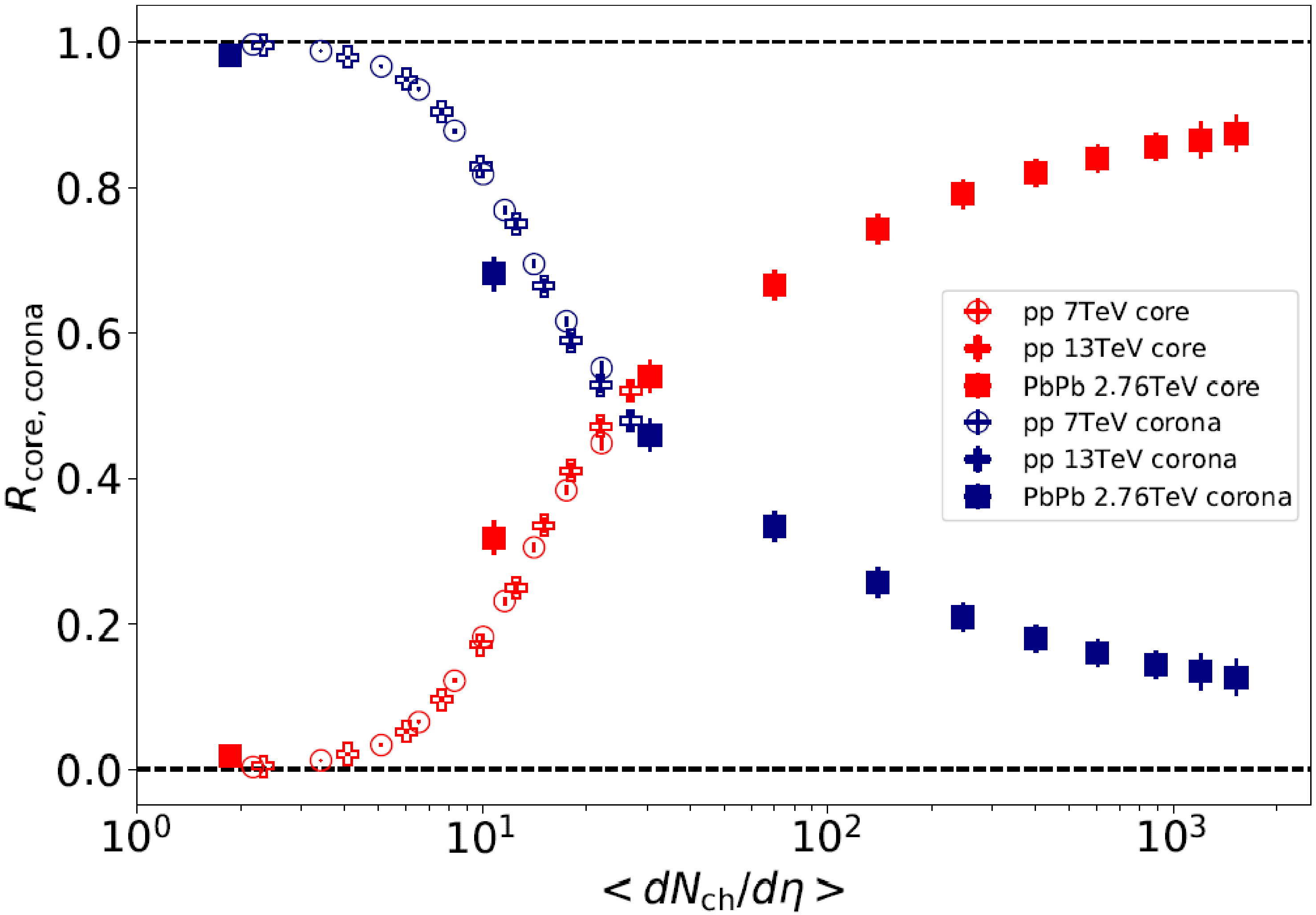

<u>According to DCCI2</u>

$$R_{\mathbf{core}} \sim \mathbf{0.5}$$

in high-multiplicity p+p collisions at $\sqrt{s} = 13$ TeV